Wireless Networks

Miao Wang
Ran Zhang
Xuemin (Sherman) Shen

Mobile Electric Vehicles

Online Charging and Discharging

Springer

Wireless Networks

Series Editor
Xuemin Sherman Shen
University of Waterloo
Waterloo, Ontario, Canada

More information about this series at http://www.springer.com/series/14180

Miao Wang • Ran Zhang • Xuemin (Sherman) Shen

Mobile Electric Vehicles

Online Charging and Discharging

Springer

Miao Wang
University of Waterloo
Waterloo, ON, Canada

Ran Zhang
University of Waterloo
Waterloo, ON, Canada

Xuemin (Sherman) Shen
University of Waterloo
Waterloo, ON, Canada

Wireless Networks
ISBN 978-3-319-25128-8 ISBN 978-3-319-25130-1 (eBook)
DOI 10.1007/978-3-319-25130-1

Library of Congress Control Number: 2015957055

Springer Cham Heidelberg New York Dordrecht London

Printed on acid-free paper

Springer International Publishing AG Switzerland is part of Springer Science+Business Media (www.springer.com)

Preface

Coordinated charging is an effective charging plan for electric vehicles (EVs) to improve the overall system energy utilization and avoid overload in an electric power grid. Besides, the stored energy and controllable loads in EVs can be discharged to the grid to help smooth the voltage and frequency fluctuations, which, for example, may be introduced by distributed generators (DGs). Either to avoid overloading or to regulate the power grid, most existing charging/discharging plans emphasize on temporal charging/discharging coordination for parked vehicles. However, for vehicles on the move, spatial coordination can also bring huge benefits to the grid. With spatial coordination, the range anxiety problem for individual EVs should be carefully handled to solve the tension between the stored energy level and the travel cost to reach the charging station. Otherwise, some EVs may be assigned to the charging stations beyond reach due to the limited battery levels.

By exploiting both spatial and temporal coordinations, we introduce an online charging/discharging strategy considering range anxieties for mobile EVs. Specifically, to collect the real-time information required by the proposed strategy, a heterogeneous wireless infrastructure is proposed by combining wide-coverage cellular networks with economic high-rate vehicular ad hoc networks (VANETs). This monograph begins with introducing the impacts of EVs on the smart grid in Chap. 1. Then, the EV charging/discharging issues and challenges are identified in Chap. 2. In Chap. 3, a mobility-aware coordinated EV charging strategy is proposed for VANET-enhanced smart grid, which not only improves the overall energy utilization with overload avoidance, but also addresses the range anxieties of individual EVs by reducing the average travel cost. Due to the equipped bidirectional chargers on EVs, vehicle-to-vehicle (V2V) charging can be enabled where energy can be directly transferred from EVs with surplus energy to other EVs with energy demand at an aggregator. In this way, the heavy power EV charging demands can be offloaded from the power grid for overload avoidance. In Chap. 4, a semi-distributed online V2V (dis)charging strategy at a swapping station based on price control is proposed to relieve the charging overload problem in the power system during peak-demand hours. In the V2V (dis)charging strategy, EVs with

sufficient energy can help to charge the demanding EVs for balancing the supply and demand at the aggregators in the smart grid. Conclusions and future directions are provided in Chap. 5.

Waterloo, ON, Canada
July 2015

Miao Wang
Ran Zhang
Xuemin (Sherman) Shen

Acknowledgments

The authors wish to acknowledge the financial support of Natural Sciences and Engineering Research Council of Canada (NSERC), Collaborative Research and Development (CRD) Grants, Canada.

The authors would like to express their sincere gratitude to Professor Weihua Zhuang and Professor Jon W. Mark for the invaluable and constant guidance throughout the study and research. We are thankful to all the members and colleagues in the Broadband Communications Research Group, University of Waterloo, for their valuable discussions and insightful suggestions, ideas, and comments.

Special thanks are also due to the staff at Springer Science+Business Media: Susan Lagerstrom-Fife and Jennifer Malat, for their help throughout the publication preparation process.

Contents

Chapter 1
Introduction

The awareness, that significant global warming is being caused by vehicle emissions, is encouraging the transport sector to adopt plug-in electric vehicles (PEVs). As reported in [1, 2], PEVs, as a promising component of sustainable and eco-friendly transportation systems, have received considerable attention recently. The introduction of PEVs into the transport sector can reduce the consumption of conventional energy sources (e.g., gasoline) and the environmental pollution (e.g., greenhouse gas emissions). As reported from industry [1], battery powered EVs, which completely leverage rechargeable batteries and thus produce no emissions, can reduce the overall emissions from the transport sector by 70 %. As such, EVs are being accounted for higher market share in the transport sector. According to the report of Electric Power Research Institute (EPRI) [2], by the year 2020, 2030, and 2050, the EV penetration level can reach 35 %, 51 %, and 62 %, respectively.

1.1 Introduction to the Smart Grid

The rapidly increasing demand of energy from all over the world imposes huge burden upon existing energy resources and power grid, resulting in an exponential increase in environmental pollution and global warming. To reduce the overall environmental pollution, renewable energy resources as an important supply alternative have become increasingly attractive by generating energy from solar, photovoltaic, wind, and so on. Using such non-conventional and renewable energy sources, distributed generations (DGs) are imposed into power grid, which can be connected locally at the distribution system level. Due to the increased penetration of DGs, to improve the efficiency, reliability, and sustainability in the production and distribution of electricity in a power grid, a smart grid has been investigated by exploiting communication technologies to gather and respond to the information of the behaviours of the suppliers and consumers. Meanwhile, with the increased

M. Wang et al., *Mobile Electric Vehicles*, Wireless Networks,
DOI 10.1007/978-3-319-25130-1_1

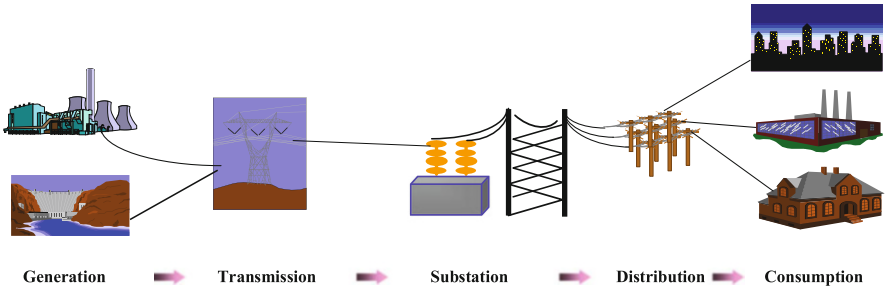

Fig. 1.1 Architecture of power grid

penetration of renewable energy sources in DGs, the power quality, reliability and security standards, power electronic interfaces and controls need to be studied in the smart grid. Specifically, due to the instability of the renewable energy supply, fluctuations on frequency and voltage at buses are introduced into the smart grid.

In the existing power grid, the main components are shown in Fig. 1.1. Generations are the resources to generate the energy for the whole systems. Through transmission, substation, and distribution parts, energy can be delivered to the customer ends. The existing electricity power grid is unidirectional based on one-way communication system. Due to the one-way communication system in the existing power grid, the utilities or generations do not take corrective actions based on the information received from the meters. Thus, there are many challenging issues in the existing power grid, including generation diversification, demand response, and the problem of carbon footprint, and so on.

To tackle the above problems, the next-generation electricity grid is introduced, also known as the "smart grid" or "intelligent grid", which integrates smart meters, distributed control and a two-way communication system to the meters as well as the ability to correct the customers' parameters. In smart grid, all the technologies, concepts, topologies, and approaches of generation, transmission, and distribution can be included, and furthermore the pervasive control and monitoring can be provided. To enable the control and monitoring on the grid operations, the smart grid is emerging as a convergence of information technology and communication technology with power system engineering.

Specifically, for the generation part in smart grid, cleaner and more efficient bulk generation technologies will be considered. Through the transmission, high quality sources of renewable energy can be accessed; wide area disturbances can be minimized; and the congestion can also be addressed in future smart grid. Accommodating new end user technologies and increased consumer participation will be included in the distribution part, for example, PEVs, DGs, smart loads, and microgrids. And for the end users, more efficient and smarter load management or distributed generation can be integrated, e.g., the PEVs as a very important component for both energy storage and controllable loads in smart grid.

PEVs with energy storage and controllable loads can be used to help the grid to compensate the fluctuating electricity generation at DGs via renewable sources. The stored energy in some PEVs can be discharged for the load demand and/or to charge other PEVs, leading to less requirements in terms of extra storage devices. Specifically, via the bi-directional charger, PEVs are capable of not only drawing energy from the power grid with the plug-in function (i.e., charging via grid-to-vehicle (G2V)), but also delivering the energy back to the grid (i.e., discharging through vehicle-to-grid (V2G)). Via V2G, discharged energy from the PEVs can help to regulate the frequency and voltage of the grid. Furthermore, through interaction among PEVs, an aggregator can perform a coordinated control for a group of PEVs for charging and discharging purposes, that is, energy can be transferred among PEVs in swapping stations [3], i.e., vehicle-to-vehicle (V2V) charging/discharging.

1.2 An Overview of EVs and Smart Charging in Smart Grid

PEVs have become a promising component of sustainable and eco-friendly transportation systems, and have received increasing attention recently. Motivated by the significant commercial and environmental potentials, prominent industrial corporations have launched products of many kinds of PEVs. For example, Tesla Motors produce a pioneer retail EV, e.g., TESLA Model S, which only costs $30 per 100 km while a common premium sedan costs $173 per 100 km [4]. In total, there are mainly three kinds of electric vehicles as follows,

- Battery electric vehicle: completely depend on the rechargeable battery.
- Hybrid electric vehicle: combine internal combustion engine with an electric motor and battery. The battery is charged by utilizing energy from regenerative breaking.
- Plug-in hybrid electric vehicle: use gas and an external power outlet to charge the battery. Plug-in hybrid electric vehicles run on battery for the first few miles and then switch over to hybrid mode as a hybrid electric vehicle.

However, the widespread adoption of PEVs brings new challenges to the grid operation for electric vehicle charging. The National Electric Code (NEC) has classified the charging level of PEVs into three types:

- Level-1: Standard 120 V. The charging duration is from 6 to 15 h. The maximum power falls between 1.44 and 1.92 kW.
- Level-2: 208–240 V. The charging duration is 2–5 h, and the maximum charging power is 7.2 kW.
- Level-3: 440/480 V. This allows very fast charging, and the charging duration can be 15–30 min.

High PEV penetration levels will lead to overload charging problems for the smart grid. For example, electric taxi charging, which is very likely to coincide with

the peak demand time of the power system, can lead to an overload of power consumption in a distribution feeder, resulting in power system instabilities in voltages and thus reduction in the energy utilization [5]. The situation is even severe for fast PEV charging as it requires much higher power than the regular charging.

Many works have been done on the impacts of PEV charing and discharging on the power system. Usually, EV charging coincides with the overall system peak hours, leading to an overload problem in power grid [6, 7]. By using a smart charging device, the overload problem can be prevented in smart grid [8]. In addition, PEVs can significantly increase the uncertainties in the demand side and reduce the life time of bues/feeders and the transformer [9]. An uncoordinated PEV charging is shown in [10] in terms of system peak load, losses and voltage drops in power grid. The above challenges, e.g., avoiding the overload, (and potential benefits, e.g., regulating the frequency) can be better addressed (and exploited) through coordinated charging/discharging strategies. By applying coordinated charging strategies, the peak load, losses and the impacts of uncoordinated charging process can be reduced in [11]. The optimal and maximum penetration of PEVs in the transportation sector of Ontario is considered based on the proposed model in [12]. Moreover, the vehicle emissions between the conventional and hybrid electric vehicles are compared in [13]. However, so far, most of the existing works have focused on the temporal coordination. Most of the works distribute the charging/discharging decisions in the power system over different time periods. Temporal coordination is performed for a group of PEVs that are assumed to be ready for charging/discharging within a specific area (e.g., parking lots or residence areas). In practice, PEVs may need fast charging when moving on the road (e.g., electric taxis). In addition, mobile PEVs can contribute to a V2G or V2V transaction if a high revenue is expected. Thus, better results can be achieved by combining the temporal information with the spatial coordination for mobile PEV charging/discharging.

In the spatial coordination of mobile PEVs, the charging/swapping station that is assigned for the PEV may be too far to reach given the PEV's current location and battery energy level (i.e., range anxiety which presents the tension between the PEV travel cost[1] and battery energy level), making the PEV battery depleted on the way, lowering the discharging revenues or increasing the charging costs. Therefore, drivers prefer charging/swapping stations at locations with less travel cost, more discharging revenue or less charging costs while considering range anxieties. However, such preference may conflict with the system technical constraints. Therefore, new online charging/discharging strategies are desired to consider both drivers' preferences and system constraints.

[1] In this monograph, the PEV energy consumed on the road to reach a charging/swapping station is referred to as the travel cost.

1.3 An Introduction of VANETs

Vehicular ad hoc networks (VANETs) have recently emerged as a prominent technology which provides revolutionary broadband services to vehicles. By deploying wireless access points such as road side units (RSUs) along highways/sidewalks and equipping vehicles with on-board communication facilities (e.g., on-board units (OBUs)), two communication types are supported for the mobile vehicles, i.e., vehicle-to-RSU (V2R) communications and vehicle-to-vehicle (V2V) communications, alternatively known as vehicle-to-infrastructure (V2I) communications and inter-vehicle communications, respectively. Within this framework, abundant applications are supported such as road safety applications (e.g., accident warning, traffic alerts), traffic monitoring/management, and infotainment delivery (e.g., video streaming, online gaming) [14, 15].

For the dedicated use of automotive applications via VANETs, the program, Vehicle-Infrastructure Integration (VII) [16], also known as IntelliDrive by the U.S. Federal Communications Commission (FCC), has allocated an exclusive 75 MHz spectrum in the 5.9 GHz band. This spectrum became known as Direct Short-Range Communications (DSRC)[2] [14]. The DSRC signals can reach a range of 1 km under the permitted power levels at data rates from 6 to 27 Mbps. The community also specifies the corresponding developing DSRC standards, including the technical details on the PHY and MAC layers and the communication architecture, which envisaged ad hoc communications among OBUs in vehicles and RSUs. In VANETs, the RSUs function as data repositories or repeaters. Specifically, with VANETs, safety applications can be obtained based on DSRC to warn drivers about potentially confliction situations based on the information received from neighboring vehicles or the RSUs directly.

Attributed to the huge potentials of VANETs in safety applications, on February 3rd, 2014, the U.S. Department of Transportation's (DOT) National Highway Traffic Safety Administration (NHTSA) announced that it would undertake to enable V2V communications to let vehicles talk with each other and ultimately avoid crashes altogether by exchanging basic safety data [17]. Moreover, motivated by the tremendous commercial potentials, pioneering industrial companies have also launched multiple projects to promote vehicular communications. For instance, "Toyota Friend" established a private mobile social network for the Toyota car owners [18].

The vehicular environment introduces unique opportunities and challenges as well as requirements. For example, new challenges can be imposed by high vehicle velocity and highly dynamic channel conditions for transmission. However, particularly for the highly mobile environments, an entirely new paradigm for vehicle

[2]DSRC protocol supports both RSU-to-vehicle/vehicle-to-RSU (R2V/V2R) and vehicle-to-vehicle (V2V) communication.

safety applications can be established, and even other non-safety applications can significantly improve the road and vehicle efficiency.

Applications of VANETs: In general, VANETs applications can be categorized into two major groups: (1) safety related applications that increase vehicle safety on the roads; (2) non-safety related applications that provide value-added services, e.g., vehicle navigation or path planning via vehicular networks.

At the most basic level, the objective of inter-vehicular safety application is to alert the potential danger on the move, by sharing current vehicular positions, velocities, and accelerations. This can soon become realistic as most of the retail vehicles nowdays are equipped with sensors to measure velocities and accelerations and with transceivers to support the V2R and V2V communications.

The other kind of application is non-safety related application, e.g., comfortable-driving applications. In this type of application, information is collected and shared in a cooperative way within a large area, e.g., in a highway network or an urban road network. One typical application is the VANET-based sensing data-sharing systems, which can provide distributed sensing data about the traffic conditions of an entire city. The information can then be utilized to regulate the vehicle traffic and cut down the individual vehicle travel time in the whole network.

Characteristics of VANETs: VANET is a special case for mobile ad hoc networks (MANETs), where the vehicles with high mobility equipped with OBU communication devices can communicate with other vehicles or the deployed infrastructure (e.g., RSUs) as shown in Fig. 1.2. Compared to the general MANETs, VANETs have unique characteristics.

1. *Rapid change in topology:* Since vehicles are highly mobile, the topology of VANETs presents frequent and rapid changes, and the trajectories of vehicles usually follow the geometric topology of freeways or the street patterns in the real world.
2. *No power constraint:* Since the batteries in the vehicles are self-chargable, vehicular communications in VANETs are not limited by the conventional power constraints like those for the hand-held devices in MANETs.

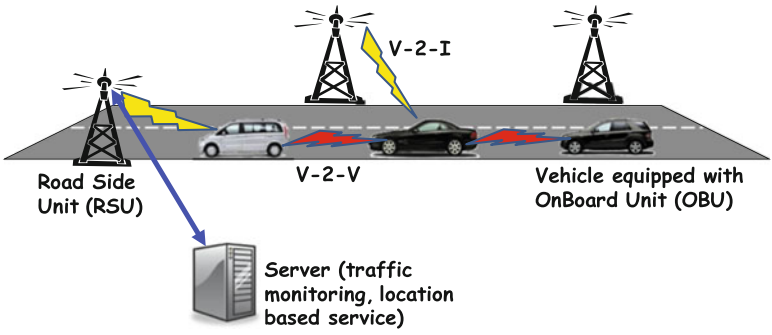

Fig. 1.2 Architecture of VANETs

3. *Large scale:* A VANET consist of a large number of vehicles, with the scale of the number of vehicles approximately 10^7 in reality [19].
4. *Variable network density:* The number of vehicles in one area is both temporally and spatially diverse, e.g., roads in the rush hours around downtown are more congested than other places or the other times of a day.
5. *High predictable mobility:* The vehicle velocities in urban areas usually ranges from 0 to 60 km/h, while the average velocity can reach up to 100 km/h on a highway. Thus, the vehicle mobility is regulated by the road patterns.

Challenges of VANETs: Most of the VANET applications, such as the Internet-based VANET applications (i.e., emailing, vehicular video conference, and traffic monitoring, etc.), lean upon the connections to RSUs for communicating with the remote servers. Such connections rely on multi-hop V2V relaying and V2R communications. While having a bright future ahead, enabling efficient vehicular communications faces fundamental challenges.

The first key challenge is network connectivity, which is challenged by the high mobility of vehicles. In general, most Internet-based VANET applications (e.g., vehicular video conferencing and traffic monitoring) rely on connections to remote Internet servers through RSUs. To extend the limited communication range of V2R communications, inter-vehicle relaying is typically exploited based on V2V communications. For example, consider an uplink scenario of VANETs,[3] vehicles help each other to relay data towards RSUs, which can then wiredly forward the received data to the remote server [20]. However, due to the high mobility of vehicles and the resultant dynamic topologies, the transient and intermittent connections among vehicles may lead to highly unreliable transmission performance for inter-vehicle transmissions.

The second challenge rises from the large scale of the vehicular network. As the quality of applications closely depends on the number of vehicles competing for transmissions and the availability of RSUs, the investigation on how nodal throughput scales with the vehicle population and RSU deployment patterns in VANETs (i.e., asymptotic network throughput capacity [21]) is essential in adopting appropriate network mechanisms (e.g., MAC protocols or relay selection schemes) as well as guiding network planning in practical (e.g., RSU deployment).

Mobility in VANETs: Almost since the advent of the prominent symbol of the twentieth century, i.e., the automobile, scientists and engineers have been making efforts to understand and model vehicular mobility patterns. The study has been made even more critical with the wide popularity of the personal automobile and the outbreak of the first traffic congestions. In the middle twentieth century, a new research field known as traffic theory comes into being aiming to understand the linkage among the traffic speed, flow, and density for efficiently dimensioning

[3] In VANETs, many basic applications are supported in uplink scenario, such as data uploading, email transmission, road traffic reporting, and environment monitoring.

the transport infrastructures and helping tackle the traffic problems. With the miniaturization of processors and the development of mobile energy sources, mobility rapidly attracts ever-increasing attention. Mobility is indeed is the source of most issues in VANETs, and the corresponding modeling and understanding forms the traffic theory: to improve the dimensioning of data transport infrastructures and to solve data traffic problems. With the advent of VANET, the study on vehicular mobility is motivated for networking research.

In order to produce realistic mobility patterns, five categories are distinguished in the existing literature as a function of the scopes and characteristics:

1. Random models: Vehicular mobility is considered random and the mobility parameters, such as speed, heading directions, and destinations are sampled from random processes. A very limited interaction between vehicles exists in this category.
2. Flow models: Following the description in flow theory, single and multi-lane mobility models based on flow theory are considered from a microscopic, mesoscopic, or macroscopic point of view.
3. Traffic models: Trip and path models are depicted in this category, where either each car has an individual trip or path, or a flow of cars are assigned with trips or paths. In addition, the impact of time on the traffic models is also considered.
4. Behavioral models: Such models are not based on the pre-defined rules but rather dynamically adaptive to a particular situation by mimicking human behaviors, such as social behaviors, dynamic learning, etc.
5. Trace-based models: Mobility traces are utilized in such models in order to extract motion patterns to either create or calibrate mobility models. The survey of human behaviors is also another source of mobility information.

1.4 Architecture of VANET-Enhanced Smart Grid

To deliver the real-time information required by the PEV online charging/discharging strategy in an efficient and reliable manner, a heterogeneous wireless network is first proposed and described. Then, the heterogeneous wireless network-enhanced smart grid architecture is shown with the objective to support the spatially and temporally coordinated charging/discharging strategy for PEVs.

1.4.1 The Heterogeneous Wireless Network

In the literature, most of the existing works exploit cellular networks (e.g., GSM, UMTS, LTE, etc.) to deliver the information required by the PEV charging/discharging strategy [22]. Cellular networks have great advantages for wireless transmission since the base stations (BSs) have large coverage range.

However, cellular networks also have inevitable drawbacks which significantly limit their efficacy in collecting the real-time vehicle information. As cellular systems are not dedicated for vehicular communications, the data delivery services can be costly. In addition, the high volume of vehicular data may cause congestions to other cellular services, especially when the vehicle density is high.

VANETs have recently emerged as a promising technology which can provide revolutionary wireless broadband communications for vehicles. By deploying along highways/sidewalks the wireless gateways (e.g., RSUs) and equipping vehicles with on-board communication facilities (e.g., OBUs), two communication types can be achieved for vehicles on the move, i.e., vehicle-to-RSU (V2R) communications and vehicle-to-vehicle (V2V) communications.[4] As VANETs are exclusively designed for information exchange among highly mobile vehicles and RSUs in a multi-hop fashion, the required real-time information can be delivered efficiently via short-range V2V and V2R communications. Consequently, the large-volume vehicle information collection and dissemination can be much cheaper than the cellular networks. However, due to high vehicle mobility and the short-range transmission nature, VANETs suffer from intermittent connections among vehicles and RSUs, leading to considerable transmission delay for real-time information delivery. The transmission delay may further affect the effectiveness of the PEV charging/discharging decisions, since the moving PEVs will keep moving and thus consuming energy while waiting for the charging/discharging decisions. Therefore, the resultant additional travel cost incurred by the transmission delay of VANETs need to be deliberately considered.

As the cellular systems and the VANETs both have pros and cons, it is beneficial if we integrate both networks to form a heterogeneous wireless network. With such a heterogeneous network, more efficient approaches for information delivery can be designed and realized with a low-cost and low-delay communication network solution. In the following chapters, the incorporation of the heterogeneous wireless network to deliver real-time messages is discussed for the online charging/discharging strategy design.

1.4.2 Heterogeneous Wireless Network-Enhanced Smart Grid Architecture

The proposed heterogeneous wireless network-enhanced smart grid architecture is shown in Fig. 1.3, consisting of a power distribution system with distributed generators (DGs), charging stations, swapping stations, PEVs, communication access points (i.e., RSUs) along the roads, and the BSs of cellular networks.

[4]Note that, in this monograph, the term V2V is used in two different contexts, one for VANET communications among vehicles and the other for energy transfer among PEVs.

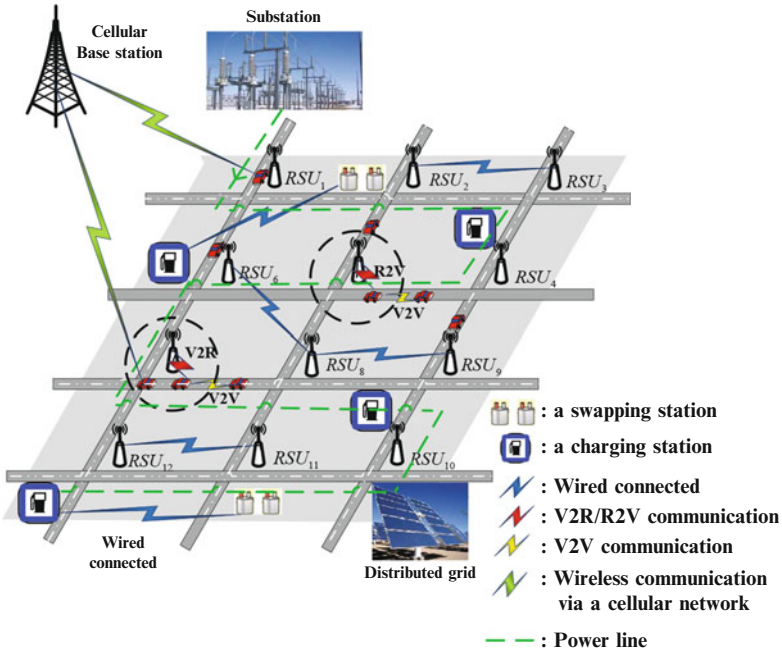

Fig. 1.3 Heterogeneous wireless network-enhanced smart grid

The power distribution system encompasses a substation and a set of DGs providing energy to the whole network through power feeders (i.e., buses). Charging stations located at different buses provide fast-charging services for all PEVs (i.e., charging via G2V). PEVs can also deliver electricity back to the grid through charging stations, i.e., discharging via V2G. Besides, PEVs can exchange energy at swapping stations without involving the power grid, i.e., charging/discharging via V2V.

The time horizon is partitioned into periods with the duration of τ. In the beginning of each period, electricity price is determined based on the collected PEV charging information and the load capacities. Similarly, based on historical readings on the remote terminal unit (RTU), the maximal power that can be exchanged at swapping stations in the following period (i.e., the load-capacity of the swapping station) can also be predicted. In the following context, denote Bus j as B_j and the load-capacity for the charging/swapping station at B_j as C_j.

A set of RSUs, denoted as $\mathbb{R}$, is deployed along the roads to gather the PEV charging/discharging information (i.e., individual charging/discharging decisions of PEVs) through V2R transmissions. Cellular BSs are also deployed in the network to support wireless communications between BSs and portable transceivers in PEVs. The RSUs and BSs are all connected through wirelines to the charging stations and able to relay the collected PEV decisions to the charging stations for updating the prices. The price is updated to balance the load capacities with the load

demands. Afterwards, when the RSUs (BSs) obtain the updated prices from the charging/swapping stations, they relay the updated price information to the PEVs through R2V and V2V transmissions or the cellular network.

Denote the set of mobile PEVs as $\mathbb{V}$. PEVs may need to be charged or be willing to discharge when moving on the roads. Each PEV is equipped with both cellular and VANET interfaces. According to certain metrics, the real-time PEV information can be either exchanged via multi-hop V2V relaying and V2R transmission or delivered to a cellular BS through the installed portable transceivers. Based on the received control messages, e.g., the price control message, the charging or discharging decisions are made by individual vehicles while considering their range anxieties. The charging or discharging decisions encompass a charging/discharging load of PEV v at bus B_j in period k (denoted as $P_{v,j,k}$) and a charging/discharging indicator indicating whether PEV v will go to the charging/swapping station at bus B_j in period k for charging/discharging (denoted as $x_{v,j,k}$). The variable $x_{v,j,k}$ is set to 1 when PEV v will be charged/discharged at B_j in period k, otherwise it is set to 0. Note that if PEV v decides to be charged, the charging load $P_{v,j,k} > 0$; reversely, when PEV v decides to be discharged, the charging load $P_{v,j,k}$ is negative. After the PEVs have made the charging/discharging decisions, the decisions are in turn delivered back to the charging/swapping stations via the heterogeneous wireless network.

1.5 Aim of This Monograph

To this end, in this monograph, we focus on leveraging the real-time vehicle information to design an efficient and efficient online PEV charging/discharging strategy with both spatial and temporal coordinations. Specifically, three underlying essential problems will be investigated: (1) What kind of information is required to support the spatially and temporally coordinated online charging/discharging strategy? (2) How to efficiently and reliably obtain the real-time information for the PEV online charging/discharging strategy? and (3) Based on the collected real-time information, how to design the mobility-aware coordinated PEV charging/discharging strategy to improve the overall power utilization and reduce the PEV charging/discharging cost?

To answer these three questions, in this monograph, we study a smart grid involved PEV fast charging system with enhanced communication capabilities, i.e., a VANET-enhanced smart grid. It exploits VANETs or VANETs-involved heterogeneous networks to collect vehicle mobility information and dispatch the charging/discharging decisions in a real-time manner. Then, we propose a mobility-aware coordinated fast charging strategy for EVs, which not only improves the overall energy utilization while avoiding power system overloading, but also addresses the range anxiety problems of individual EVs by reducing the average PEV travel cost. In addition, to make EV charging more efficient in a smart grid, a vehicle-to-vehicle energy swapping strategy is further proposed to offload the heavy

EV charging load from the smart grid to the swapping station, aiming to (i) relieve the EV charging burden for the power grid by stimulating EVs with surplus energy to participate in EV charging, and (ii) to maximize the revenues for discharging EVs and minimize the cost for charging EVs.

References

1. A comprehensive guide to plug-in hybrid vehicles, Hybrid Cars (2011), [Online] available: http://www.hybridcars.com/plug-in-hybrid-cars/#battery
2. Electric Power Resech Institute, [Online] available: http://www.epri.com/Pages/Default.aspx
3. C. Liu, K. Chau, D. Wu, S. Gao, Opportunities and challenges of vehicle-to-home, vehicle-to-vehicle, and vehicle-to-grid technologies. Proc. IEEE **101**(11), 2409–2427 (2013)
4. TESLA Motors, [Online] available: http://www.teslamotors.com/Pages/goelectric#
5. P. Richardson, D. Flynn, A. Keane, Local versus centralized charging strategies for electric vehicles in low voltage distribution systems. IEEE Trans. Smart Grid **3**(2), 1020–1028 (2012)
6. G.T. Heydt, The impact of electric vehicle deployment on load management strategies. IEEE Trans. Power Appar. Syst. **1**(144), 1253–1259 (1983)
7. A. Heider, H.J. Haubrich, Impact of wide-scale EV charging on the power supply network, in *IEEE Colloquium on Electric Vehicles – A Technology Roadmap for the Future*, London, vol. 6, no. 262, 1998, pp. 1–4
8. K. Schneider, C. Gerkensmeyer, M. Kintner-Meyer, M. Fletcher, Impact assessment of plug-in hybrid electric vehicles on Pacific Northwest distribution systems, in *IEEE Power and Energy Society 2008 General Meeting*, Pittsburgh, US 2008
9. C. Roe, F. Evangelos, J. Meisel, S. Meliopoulos, T. Overbye, Power system level impacts of PHEVs, in *Proceedings of the 42nd Hawaii International Conference on System Sciences*, Waikoloa, US 2009
10. K. Clement-Nyns, E. Haesen, J. Driesen, The impact of charging plug-in hybrid electric vehicles on a residential distribution grid. IEEE Trans. Power Syst. **25**(1), 371–380 (2010)
11. K. Clement, E. Haesen, J. Driesen, Coordinated charging of multiple plug-in hybrid electric vehicles in residential distribution grids, in *Proceedings of the Power Systems Conference and Exposition*, Seattle, US 2009
12. A. Hajimiragha, C.A. Canzares, M.W. Fowler, A. Elkamel, Optimal transition to plug-in hybrid electric vehicles in Ontario, Canada, considering the electricity-grid limitations. IEEE Trans. Ind. Electron. **57**(2), 690–701 (2010)
13. C.H. Stephan, J. Sullivan, Environmental and energy implications of plug-in hybrid-electric vehicles. Environ. Sci. Technol. **42**(4), 1185–1190 (2008)
14. L. Cheng, B.E. Henty, D.D. Stancil, F. Bai, P. Mudalige, Mobile vehicle-to-vehicle narrow-band channel measurement and characterization of the 5.9 GHz dedicated short range communication (DSRC) frequency band. IEEE J. Sel. Areas Commun. **25**(8), 1501–1516 (2007)
15. H.T. Cheng, H. Shan, W. Zhuang, Infotainment and road safety service support in vehicular networking: from a communication perspective. Mech. Syst. Signal Process. **25**(6), 2020–2038 (2011)
16. Vehicle Infrastructure Integration (VII) Program, http://www.vehicle-infrastructure.org/
17. http://www.nhtsa.gov/
18. Toyota Friend by Toyota, http://pressroom.toyota.com/releases/toyota+friend+social+network.htm
19. Y. Khamayseh, M. Yassein, M. Alghani, C. Mavromoustakis, Network size estimation in VANETs. Netw. Protoc. Algorithms **5**(3), 136–152 (2013)

20. M. Abboud, L. Jaoude, Z. Kerbage, Real time GPS navigation system (2004), http://webfea-lb.fea.aub.edu.lb/proceedings/2004/SRC-ECE-27.pdf
21. M. Grossglauser, D. Tse, Mobility increase the capacity of ad hoc wireless networks. IEEE/ACM Trans. Netw. **10**(4), 477–486 (2002)
22. L. Gan, U. Topcu, S. Low, Optimal decentralized protocol for electric vehicle charging. IEEE Trans. Power Syst. **28**(2), 940–951 (2013)

Chapter 2
Charging/Discharging for EVs

Several studies have demonstrated that the power system can be significantly impacted by the high penetration levels of PEV charging. Other the other hand, coordinated discharging contains tremendous benefits to the grid. In order to efficiently implement such design principles, many challenging issues exist which include PEV mobility modeling, transmission network selection, tradeoff balancing between the power system technical limitations and drivers' preferences, and the business revenue modeling for V2G and V2V transactions.

2.1 Classifications of Charging/Discharging Strategies

The research works on charging/discharging strategy design for PEVs in the smart grid can be categorized from different perspectives as follows:

- Centralized and decentralized strategies (e.g., [1]): In centralized strategies, the charging/discharging strategy is performed by a centralized controller. The globally optimal solutions can be achieved, but with high signaling overhead for information collection and high computation requirements. In the decentralized strategy, the decisions are made locally by the PEVs with an iteration-based approach. Iterative information exchange is required, but with reduced computation complexity. In this monograph, with the help of VANETs in real-time information deliver and computationally powerful remote traffic server, we propose centralized charing/discharging strategy to obtain globally optimal performance, as detailed in Chap. 3.
- Pure PEV coordination (e.g., [1]) and price control-based strategy (e.g., [2]): In pure PEV coordination, drivers are assumed to unconditionally follow the charging decisions. However, for mobile PEVs, such decisions may cause a conflict between the system technical limitations and the drivers' preferences. On the contrary, price control based strategy can effectively address such a

M. Wang et al., *Mobile Electric Vehicles*, Wireless Networks,
DOI 10.1007/978-3-319-25130-1_2

problem. The charging/discharging decisions are made based on the electricity prices, which are jointly determined by the charging stations based on the potential demands/supplies from PEVs' charging/discharging decisions. In this monograph, we propose a strategy based on price control in Chap. 4, by which a driver is stimulated to follow the coordinated decision due to a lower electricity price for charging or higher revenue for discharging.

- Myopic (e.g., [3]) and predictive (e.g., [4]) charging/discharging strategies: The myopic charging/discharging strategies are based only on the current information in the grid, while in a predictive strategy, the future power demands in the grid are also considered when making the charging/discharging decisions. Since predictive charging/discharging strategies consider the effects of both current and future PEV charging/discharging loads on the power grid, the charging/discharging decisions through short-term prediction of power loads are more reliable in reality. Therefore, in this monograph, a predictive charging/discharging strategy is proposed in Chap. 3.

2.2 Electric Vehicle Charging Strategy Design

Up to now, many studies have shown that the power system can be significantly affected by the high penetration levels of EV charging [5, 6]. To prevent the power system from being overloaded during the peak time, load management strategies are needed to distribute the EV charging load over both time and space [7]. In [1, 8], to avoid power system overloading and improve the load factor of the whole system, the peak load is shifted to off-peak periods. In [9, 10], it is demonstrated through comparison that the global EV charging strategies which coordinate the charging duration and rates of multiple EVs based on the global load information outperform the local strategy in terms of energy utilization. In [11, 12], the spatial diversity of EV charging is incorporated, modeled and evaluated to further help regulate the charging profile. However, most of the existing EV charging strategies assume EVs to be stationary when they need charging. Few works take into account the vehicle mobility, which is non-neglectable since it is the most important feature of a vehicle, especially for fast-charging applications. Due to the vehicle mobility, range anxiety, i.e., the tension between the travel cost and the EV battery level, is key to the feasibility of the charging decisions. Therefore, new efficient EV charging strategies are desired to leverage the real-time vehicle mobility information to solve the range anxiety problem.

To obtain the real-time vehicular information, most existing works rely on cellular or Wi-Fi systems [13–15]. However, these systems have inevitable drawbacks which limit their practicability in collecting the vehicle information. First, for dense vehicular networks, the inaccuracy of the location measurement in both systems [16] may significantly degrade the charging performance. Second, as cellular systems are not exclusive systems for vehicular communications, the collection services can be highly costly, and the high volume of vehicular data transmission may probably

cause congestion for other cellular services especially in a high-density vehicular scenario; besides, the short coverage for the Wi-Fi systems may cause large latency in information delivery, and delivery ratio may be dramatically reduced due to the high mobility of vehicles.

Thanks to VANETs, the real-time message can be delivered much faster, cheaper and more efficiently than the above systems, especially for dense and highly mobile vehicular environment [17]. Exclusively designed for information exchange among highly mobile vehicles and RSUs, the supported short-range V2V and V2R communication effectively expands the transmission range of vehicles in a multi-hop manner with higher data rates. As information can be shared among the RSUs wiredly and be relayed through V2V transmissions, higher throughput and delivery ratio as well as lower delay can be realized for the large volume of vehicle information exchange [18, 19]. All these facts make it possible to perform centralized coordinated charging strategy for a group of vehicles. Thus, VANETs are exploited in a smart grid to support the real-time information collection. The range anxiety which captures the tension between the travel cost and the current vehicle battery level can be introduced as additional constraints to ensure the viability of the charging decisions.

Therefore, with real-time vehicle information collection and decision dissemination via VANETs, our objective in this monograph is to design mobility-aware coordinated EV charging/discharging strategies, with considering the range anxieties, energy utilization improvement, and travel cost reduction.

2.3 Challenging Issues for Charging/Discharging Strategy Design

2.3.1 Mobility Modeling of PEVs

The mobility model of PEVs has a direct impact on the travel cost to a charging/swapping station and further affects the coordinated PEV charging/discharging decision making. Consider that PEVs are running on the roads in a suburban area following a certain mobility model, e.g., Wiedemann 74 [20]. The mobility of each PEV can be characterized by random variables (S, λ). The notation S denotes the vehicle velocity, which takes n possible values. When $n = 2$, S has two states: a lower velocity S_L and a higher velocity S_H. The transition between the two states is modeled into a two-state continuous Markov chain with state transition rates, λ_{LH} or λ_{HL}, respectively. The model can be exploited to depict the human driving behaviors in reality, i.e., a driver usually drives at a velocity for a period and then changes to another velocity according to his/her will, the road conditions, or the headway distance between the vehicle and the vehicle in front. With the n-state continuous Markov chain of the Wiedemann 74 model, the headway distance between two

neighboring PEVs in one lane, inter-contact time among PEVs, and vehicle-density, etc., can be derived, which serve as intermediate results for calculating the travel cost and the energy consumed due to the transmission delay.

With the mobility model and the calculated travel cost and transmission delay, the range anxiety can be specified.

2.3.2 Network Selection for Real-Time Information Delivery

In VANETs, the high PEV mobility and the short-range transmission nature result in intermittent V2V and V2R connections, which further bring about a transmission delay and thus incur an additional travel distance (cost) while PEV v is waiting for the charging decisions from VANETs. On the other hand, leveraging the cellular network for information delivery may incur additional monetary cost. Thus the network selection mechanism need to be developed to balance the tradeoff between the travel cost due to transmission delay in VANETs and the monetary cost mainly due to the cellular networks.

Denote the travel distance for PEV v in period k while waiting for a decision from VANETs as $d_{v,k}$. Based on the mobility model of PEVs described above, the travel distance, $d_{v,k}$, can be calculated as $d_{v,k} = \psi(S, \lambda, \zeta, R, L, \pi)$, where $\psi(\cdot)$ is a function that measures the impact of transmission delay in VANETs on the travel distance $d_{v,k}$. The transmission delay in VANETs decreases with

1. the vehicle velocity S and the inverse of the parameter $\frac{1}{\lambda}$, since increasing S and $\frac{1}{\lambda}$ will reduce the average number of hops in a multi-hop transmission link, thus leading to a reduced transmission delay,
2. the vehicle density (i.e., ζ), since increasing the vehicle density will create more chances for a successful transmission, thus potentially reducing the average transmission delay for a multi-hop communication link,
3. higher possibility for V2R transmissions in the network (i.e., larger transmission range R or more deployed RSUs to decrease the average inter-RSU distance L), and
4. a more efficient transmission mechanism π, e.g., choosing the farthest vehicle within its transmission range as the relay to reduce the potential number of transmission hops, or designing a more efficient MAC protocol to avoid transmission collisions among multiple transmission pairs.

The travel cost due to the transmission delay in VANETs is defined as a linear non-decreasing function $PC(d_{v,k})$ to measure the travel cost $P_{cost}^{v,k}$ in terms of energy for PEV v to wait for the decision in period k.

By balancing the VANET travel cost $P_{cost}^{v,k}$ with the cellular network monetary cost, the dynamic and adaptive network selection can make the information delivery more efficient and economic.

2.3.3 Balancing the Tradeoff Between the Power System Technical Limitations and Drivers' Preferences

In reality, drivers usually have their own preferences when choosing a charging/swapping station, e.g., for the shortest path length or the most familiar station. But there are times when the preferred charging/swapping station may not be able to support any more power loads. In such a situation, in order to avoid the power overload of the system, another charging/swapping station has to be assigned to PEV v for charging/discharging, which is referred to as spatial coordination.

In addition, based on the travel distance $d_{v,k}$, the travel cost for PEV v in period k in terms of energy, denoted as $PC(d_{v,k})$, should not exceed the discharging revenue, or the electricity price should be cheaper to motivate the drivers to go to the designated charging/swapping station. The travel cost can be also formulated based on other driver preferences (for a subset of stations along the customer route). For instance, given the driver's route, he/she will prefer to choose a charging station along that route. In such a situation, the selected charging station should be chosen from a subset of charging station candidates deployed only along that route. This subset of the charging station candidates can be incorporated into the optimization problem as an additional constraint.

Since drivers prefer to follow their preferences for charging/discharging, tradeoff exists between the optimal utilization of the power system and the drivers' personal preferences. This tradeoff unveils the challenging issues of (1) how to define the preferences of individual drivers, and (2) how to balance the tradeoff between the system technical limitations and drivers' individual preferences.

References

1. P. Richardson, D. Flynn, A. Keane, Local versus centralized charging strategies for electric vehicles in low voltage distribution systems. IEEE Trans. Smart Grid **3**(2), 1020–1028 (2012)
2. L. Gan, U. Topcu, S. Low, Optimal decentralized protocol for electric vehicle charging. IEEE Trans. Power Syst. **28**(2), 940–951 (2013)
3. Y. Cao, S. Tang, C. Li, P. Zhang, Y. Tan, Z. Zhang, J. Li, An optimized EV charging model considering TOU price and SOC curve. IEEE Trans. Smart Grid **3**(1), 388–393 (2012)
4. M. F Shaaban, M. Ismail, E.F. El-Saadany, W. Zhuang, Real-time PEV charging/discharging coordination in smart distribution systems. IEEE Trans. Smart Grid **5**(4), 1797–1807 (2014)
5. M. Shaaban, Y. Atwa, E. El-Saadany, PEVs modeling and impacts mitigation in distribution networks. IEEE Trans. Power Syst. **28**(2), 1122–1131 (2013)
6. D. Ban, G. Michailidis, M. Devetsikiotis, Demand response control for PHEV charging stations by dynamic price adjustments, in *Proceedings of the IEEE Innovative Smart Grid Technologies*, Washington, DC, Jan 2012
7. R.C. Green, L. Wang, M. Alam, The impact of plug-in hybrid electric vehicles on distribution networks: a review and outlook. J. Renew. Sustain. Energy Rev. **15**(1), 544–553 (2011)
8. G.T. Heydt, The impact of electric vehicle deployment on load management strategies. IEEE Trans. Power Appar. Syst. **1**(144), 1253–1259 (1983)

9. K. Mets, T. Verschueren, W. Haerick, C. Develder, F. Turck, Optimizing smart energy control strategies for plug-in hybrid electric vehicle charging, in *Proceedings of the IEEE Network Operations and Management Symposium Workshops*, Osaka, Apr 2010
10. K. Clement, E. Haesen, J. Driesen, Coordinated charging of multiple plug-in hybrid electric vehicles in residential distribution grids, in *Proceedings of the IEEE Power Systems Conference and Exposition*, Seattle, Mar 2009
11. L. Kelly, Probabilistic modeling of plug-in hybrid electric vehicle impacts on distribution networks in British Columbia, M. S. thesis, Department of Mechanical Engineering, University of Victoria, Victoria, 2009
12. S. Bae, A. Kwasinski, Spatial and temporal model of electric vehicle charging demand. IEEE Trans. Smart Grid **3**(1), 394–403 (2012)
13. J. Herrera, D. Work, R. Herring, X. Ban, A. Bayen, Evaluation of traffic data obtained via GPS-enabled mobile phones: the mobility century field experiment, in *Working Paper UCB-ITS-VWP-2009-8*, Aug 2009
14. R. Herring, A. Hofleitner, S. Amin, Using mobile phones to forecast arterial traffic through statistical learning, in *Proceedings of the 89th Annual Meeting of Transportation Research Board*, Washington, DC, Jan 2010
15. K. Lee, J. Lee, Y. Yi, I. Rhee, S. Chong, Mobile data offloading: how much can WiFi deliver? in *Proceedings of the ACM Co-NEXT*, New York, Nov 2010
16. H. Liu, A. Danczyk, R. Brewer, R. Starr, Evaluation of cell phone traffic data in Minnesota. Transp. Res. Rec. **2086**(1), 1–7 (2008)
17. N. Lu, N. Zhang, N. Cheng, X. Shen, J. Mark, F. Bai, Vehicles meet infrastructure: toward capacity-cost tradeoffs for vehicular access networks. IEEE Trans. Intell. Transp. Syst. **14**(3), 1266–1277 (2013)
18. M. Wang, H. Shan, L.X. Cai, N. Lu, X. Shen, F. Bai, Throughput capacity of VANETs by exploiting mobility diversity, in *Proceedings of the IEEE ICC'12*, Ottawa, June 2012
19. N. Lu, T. Luan, M. Wang, X. Shen, F. Bai, Bounds of asymptotic performance limits of social proximity vehicular networks. IEEE/ACM Trans. Netw. **22**(3), 812–825 (2014)
20. R. Wiedemann, Modeling of RTI-elements on multi-lane roads, in *Proceedings of the Drive Conference*, Brussels, Feb 1991

Chapter 3
Mobility-Aware Coordinated EV Charging in VANET-Enhanced Smart Grid

Coordinated charging can enable efficient charging for electric vehicles (EVs) to enhance the overall energy utilization while avoiding the overload of an electric power system. However, it is challenging to design an efficient coordinated charging strategy to guide the mobile EVs to fast-charging stations to achieve globally optimal energy utilization. In this chapter, we study a specific smart grid with enhanced communication capabilities, which is termed as a VANET-enhanced smart grid. Vehicular ad-hoc networks (VANETs) are leveraged therein to support real-time communications among highly mobile EVs and between EVs and road-side units (RSUs) for real-time vehicle mobility information collection and charging decisions dispatching. We then propose a mobility-aware coordinated charging strategy for EVs. The proposed strategy can not only improve the overall energy utilization while protecting the power system from overload, but also address the range anxieties of individual EVs via deliberately controlling the average travel cost. Specifically, we consider the travel cost incurred by mobility for an EV in two-fold: (1) the travel distance from the current EV location to the fast-charging station, and (2) the transmission delay for an EV to receive a charging decision through the VANETs.

3.1 Introduction

As a promising enabler for sustainable and eco-friendly transportation systems, electric vehicles (EVs) have attracted ever-increasing attention worldwide [1, 2]. Powered by electricity instead of gasoline, EVs provide great potential to save the customers thousands of dollars over the vehicle lifetime. For instance, the TESLA Model S, a pioneering retail EV produced by TESLA Motors, costs $30 per 100 kms, compared to $173 per 100 kms by a regular premium sedan [3]. Besides, the penetration of EVs into the transport sector reduces the consumption

M. Wang et al., *Mobile Electric Vehicles*, Wireless Networks,
DOI 10.1007/978-3-319-25130-1_3

of conventional energy sources (e.g., gasoline) and thus lowers the environmental pollution (e.g., carbon footprints). As reported from industry [4], battery EVs, which completely leverage rechargeable batteries and thus produce no emissions, can reduce the overall emissions from the transport sector by 70 %. As such, EVs are being accounted for higher market share in the transport sector. According to the report of Electric Power Research Institute (EPRI) [5], by the year 2020, 2030, and 2050, the EV penetration level can reach 35 %, 51 %, and 62 %, respectively.

However, the wide popularity of EVs in the transportation system may lead to charging problems for mobile EVs fully depending on rechargeable batteries. Specifically, it is very likely that the EV charging coincides concentratively with the peak demand time of the power system, thus incurring overload on a distribution feeder. As a result, system instability and decrease in overall energy utilization [6, 7] will be caused, especially for fast EV charging as much higher power than the regular charging is required. To mitigate the impact of fast EV charging on the power system, some works exploit energy storage systems, however, at an additional cost of deploying the energy storage devices [8]. Thus, to prevent the power system from overloading during the peak time and boost the energy utilization without additional deployment cost, load management strategies are proposed to coordinate the distribution of EV charging load both temporally and spatially. Meanwhile, for fast EV charging, the designated charging stations must be within the reach of mobile EVs given the current EV locations and battery levels, in order to account for the tension between the current battery levels and the travel cost to the charging stations, which is called range anxiety in this chapter.

Abundant literature [9–20] has been proposed on the strategy design for coordinated EV charging. Most of the existing works resolve problems only in the power system plane. That is, the group of EVs considered for coordinated charging are assumed to be ready for charging within an area (e.g., parking lots or residential areas). Few works have taken the vehicle-specific features, i.e., vehicle mobility, into the charging strategy in a fast-charging context. Actually, since EVs may need to be charged when running on the roads, the energy consumption on the way to the charging station, referred to as the travel cost in this chapter, should be deliberated. Otherwise, one EV may fail to reach the assigned charging station by the existing strategies given the EV's current location and battery level. Because of the range anxiety, drivers prefer to charge at locations with less travel cost. Therefore, new charging strategies are indispensable to account for the range anxieties and vehicle mobility to effectively reduce the EV travel cost. In order to track the vehicle mobility, the EV information (e.g., locations and battery levels) should be collected in a real-time manner to help charging decision making.

To this end, in this chapter, we focus on leveraging the real-time EV mobility information to help design an efficient and effective coordinated EV charging strategy, aiming at improving the overall energy utilization, reducing the average EV travel cost, and avoiding the overload of the power system. To properly design the strategy, it is essential to carefully consider: (1) how to efficiently and reliably achieve the real-time information of mobile vehicles required by the EV charging strategy; and (2) based on the collected information, how to perform mobility-aware

coordinated EV charging to improve energy utilization and reduce EV travel cost while preventing power system from overload.

Exploiting the vehicular ad-hoc networks (VANETs), the first problem can be resolved in a promising way. Exclusively designed for multi-hop information exchange among highly mobile vehicles and road-side units (RSUs), the short-range vehicle-to-vehicle (V2V) and vehicle-to-RSU (V2R) communications [21–23] supported by VANETs can enable efficient delivery of the required real-time information, making large-volume vehicle information collection cheaper and faster compared to other networks (e.g., cellular networks and Wi-Fis) [24]. Besides, RSUs can significantly improve the timeliness of data collection and dissemination, making it possible to perform coordinated charging strategies for a group of mobile vehicles [25]. Therefore, in this chapter, VANETs are incorporated into a smart grid to collect the real-time information of mobile EVs and dispatch the charging decisions. Moreover, as the energy is still consumed in moving EVs waiting for the charging decisions, the transmission delay for information exchange in VANETs will cause additional travel cost. Thus, we also conduct analysis on the transmission delay given the vehicle densities and the RSU deployment.

To tackle the second problem, the range anxieties are considered based on vehicle mobility. Specifically, a mobility-aware coordinated EV charging strategy is proposed to make charging decisions based on the historic remote terminal unit (RTU) readings of the power grid and the collected real-time vehicle information. Based on the collected information, the following issues are addressed in a coordinated fashion: (1) Given the current battery level, should a vehicle be charged in the next period; (2) which charging station should be assigned to this vehicle considering the range anxiety with its current location; and (3) how much energy should be charged to this vehicle to improve the overall energy utilization and guarantee the stability of the power system. The optimal charging problem is formulated into a time-coupled mixed-integer linear programming (MILP) problem, which is time-complicated to solve. However, by discovering the linear relationship among EV charging loads of feeders, the MILP problem is time-decoupled into a set of sub-MILPs via Lagrange duality [26]. Each sub-MILP can be further solved by the branch-and-cut-based outer approximation algorithm [27].

In summary, to handle the range anxieties of EVs, we integrate VANETs into smart grid to collect real-time vehicle information for vehicle mobility tracking (e.g., locations and battery levels). We then propose a predictive mobility-aware coordinated EV charging strategy to improve the power utilization, and reduce average EV travel cost, and prevent overload of the power system for the next charging period. The main contributions of the chapter are fourfold.

- First, the architecture of the VANET-enhanced smart grid is proposed, where VANETs enable efficient communications among mobile EVs and RSUs to collect useful information and disseminate the EV charging decisions in a real-time manner; particularly, the collected information is processed and the predictive coordinated EV charging strategy is performed in a traffic server;

- Second, considering the range anxieties of EVs, a mobility-aware coordinated EV charging strategy is designed to enhance the overall energy utilization of the power system and reduce the average EV travel cost while avoiding the overload of the power system. Particularly, the linear relationship among the EV charging loads of the charging stations is unveiled, which is essential for the load distribution; in addition, the travel cost is defined and formulated to show how EV mobility impacts the charging decision making;
- Third, the globally optimal charging problem is formulated as a time-coupled MILP problem which can be decoupled into a set of sub-MILPs exploiting Lagrange duality. Each sub-MILP can be further solved by the branch-and-cut-based outer approximation algorithm; and
- Finally, extensive simulations are conducted to validate the efficacy and efficiency of the proposed EV charging strategy. VISSIM [28] is utilized to extract the simulation traces, upon which a highly realistic suburban scenario is built. Particularly, the transmission delay caused by VANETs is fully evaluated in the studied context. Simulation results demonstrate that the proposed strategy significantly outperforms the traditional autonomous charging strategy (without VANETs) in terms of the energy utilization and the average EV travel cost.

The remainder of this chapter is organized as follows. Section 3.2 elaborates the system model. Sections 3.3 and 3.4 present the formulation and solution of the mobility-aware coordinated EV charging problem, respectively. The performance of the proposed strategy is demonstrated in Sect. 3.5 via simulations. The related works are introduced in Sect. 3.6. Section 3.7 concludes this chapter.

3.2 System Model

With the objective of providing a coordinated mobility-aware EV charging strategy based on the real-time vehicle information, a VANET-enhanced smart grid architecture is first introduced to efficiently conduct the coordinated EV charging strategy. The power system model is then depicted together with the flow formulas. At last, the mobility model, charging model and transmission model of EVs are presented.

3.2.1 VANET-Enhanced Smart Grid

Figure 3.1 gives the components of the proposed VANET-enhanced smart grid architecture. The architecture consists of a power distribution system, charging stations (e.g., at parking lots), a traffic server, RSUs along the road sides and EVs. Energy to the whole network is supplied by the power distribution system via power feeders (i.e., buses). The charging stations provide fast-charging for all the EVs.

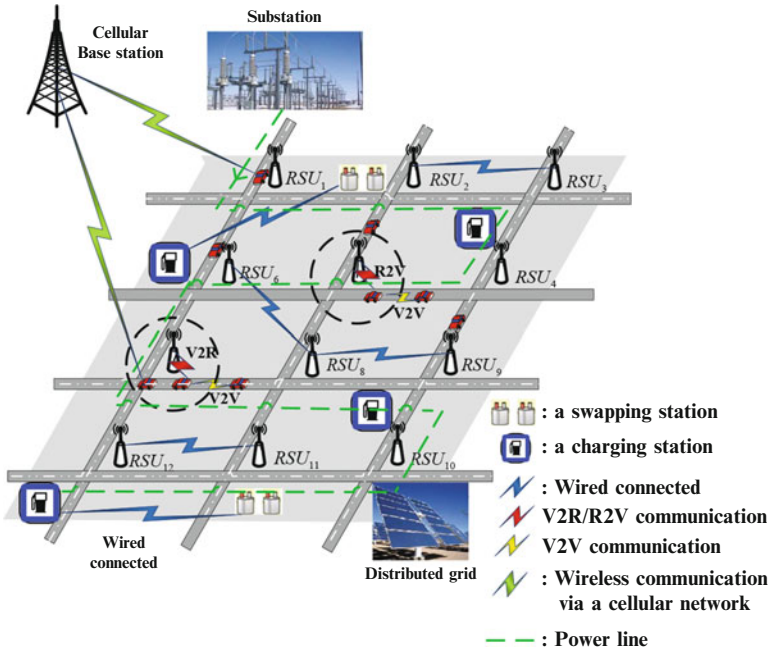

Fig. 3.1 The VANET-enhanced smart grid architecture

Based on historic RTU readings of each bus in the distribution system, the voltage at each charging station in the next period can be predicted [29]. The maximal power that can be provided by each charging station (i.e., the load-capacity of each charging station) can then be calculated. In the following text, denote as P^j_{total} the load-capacity of Bus_j. The historic readings are conveyed to the traffic server wiredly. The traffic server is in charge of performing the predictive charging strategy to make globally optimal charging decisions for the EVs that need to be charged, based on the real-time EV information from VANETs and the historic RTU readings. The strategy is conducted period by period. The charging decisions include the charging load/rate of EV v at Bus_j in period k (denoted as $Pch_{v,j,k}$) and the charging indicator of vehicle v specifying whether EV v should be charged at station j in period k (denoted as $x_{v,j,k}$). The indicator $x_{v,j,k}$ is set to 1 if EV v is scheduled for charging at Bus_j in period k, and 0 otherwise.

For the VANETs, a set of EVs are moving around in the network region following map-based paths. Denote the set of EVs as $\mathbb{V}$. EVs may need charging while moving on the roads. The real-time EV information can be exchanged among the on-board units (OBUs) equipped with vehicles, via multi-hop V2V relaying,

under the dedicated-short-range-communication (DSRC) protocol [30],[1] with the transmission range R. Besides, the Global Position System (GPS) devices, which offer the shortest-path navigation services, are also installed in EVs and wiredly connected with the OBU. In addition, a set of RSUs are uniformly deployed along roads with the capability of collecting the EV information (e.g., locations and battery levels) via V2R transmissions, based on DSRC protocol, with the transmission range R. Denoted the set of RSUs as $\mathbb{R}$. Through wireline connection to the traffic server, RSUs can relay the collected EV information to the traffic server for making the globally optimal EV charging decisions. When the RSUs obtain the EV charging decisions from the traffic server, they will relay the decisions back to the EVs through R2V and V2V transmissions.

To summarize, the VANET-enhanced smart grid system operates as follows.

- Information collection and reporting to the traffic server: The required information is two-fold: the historic RTU readings of each bus in the power system and the real-time EV information. The former is conveyed to the traffic server through wireline, based on which the charging load constraint of each charging station can be estimated; the latter is gathered via multi-hop V2V relaying and V2R transmissions;
- Decision making of the predictive coordinated EV charging: The traffic server fuses all the gathered information and makes the optimal EV charging decisions to enhance the power utilization of the grid and decrease the average EV travel cost while preventing the power system from overloading;
- Decision dissemination: Upon receiving its own charging decision from either the neighboring vehicles or the RSU, the OBU of an EV will deliver the decision to the GPS device. The GPS device will navigate the EV to the assigned charging station.

3.2.2 Power System Model

To implement predictive charging strategy for EVs in the VANET-enhanced smart grid, the power flow on the feeders need to be considered. In this subsection, a power system model is described where the relation between bus voltages and power loads is given to help derive the relation among EV charging loads on feeders.

Consider a smart grid with the system model shown in Fig. 3.1. The power system can be abstracted as a one-line diagram with multiple buses. For better illustration, an example of a 12-bus system is presented in Fig. 3.2a, b is the abstracted equivalent power system model of Fig. 3.2a. Denote the set of buses in the system as N, which is 12 in this example. Define the *generation buses* as the buses injecting power into

[1] DSRC protocol supports both RSU-to-vehicle/vehicle-to-RSU (R2V/V2R) and vehicle-to-vehicle (V2V) communication.

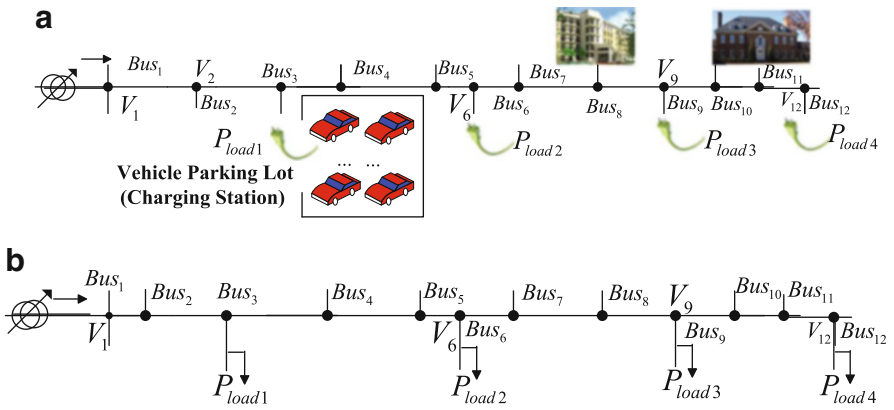

Fig. 3.2 The power system model. (**a**) Illustrated power system model. (**b**) Equivalent power system model

Fig. 3.3 The power flow illustration

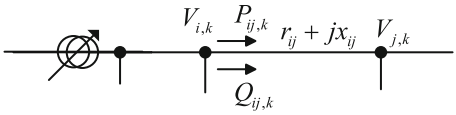

the system, i.e., Bus_1 in Fig. 3.2a, and define the others which only have load as the *load buses*, e.g., Bus_3, Bus_6, etc. The power system is supplied via the substation at the generation bus. EV charging stations are located together with load buses, e.g., Bus_3, Bus_6, Bus_9 and Bus_{12}, respectively. Each charging station is connected to the grid via a standard single-phase Alternating-Current (AC) connection. Due to the thermal limit of service cable or current rating of fuse, an EV charging station at Bus_j is constrained by the associated load capacity P^j_{total} [9]. Although there is the concept of vehicle-to-grid for a local system [10], we do not consider bi-directional flow of electricity or the directional flow from an EV battery in this chapter.

The voltages of two neighboring buses in period k, e.g., $V_{i,k}$ and $V_{j,k}$ in Fig. 3.3, can be approximated as [29]

$$V_{i,k} - V_{j,k} = \frac{P_{ij,k} \cdot r_{ij} + Q_{ij,k} \cdot x_{ij}}{V_{j,k}} \tag{3.1}$$

where $P_{ij,k}$ and $Q_{ij,k}$ are the active and reactive power flow from Bus_i to Bus_j in period k, respectively, and $r_{ij} + jx_{ij}$ is the impedance of the feeder line *i*-*j*. In per unit, (3.1) can be approximated as

$$V_{i,k} - V_{j,k} = P_{ij,k} \cdot r_{ij} + Q_{ij,k} \cdot x_{ij}. \tag{3.2}$$

Note that all the voltages of buses should stay within a certain range which is the main operation constraint of the distribution system [29]. For instance, the voltage magnitude at Bus_j in period k is bounded by an upper and lower limit $V^{\min}_{j,k}$ and

$V_{j,k}^{\max}$, respectively, i.e., $V_{j,k}^{\min} \leq V_{j,k} \leq V_{j,k}^{\max}$. It has been proved by [29] that the minimum voltage point can only occur at the end of the power line, since the only generation bus is located at the beginning of the distribution system.[2] Then the minimum voltage $V_{N,k}$ can be derived as

$$V_{N,k} = V_{1,k} - \sum_{i=1}^{N-1} [P_{i(i+1),k} \cdot r_{i(i+1)} + Q_{i(i+1),k} \cdot x_{i(i+1)}]. \tag{3.3}$$

3.2.3 EV Mobility and Charging Model

According to [31], two random variables (V, D) can be used to characterize the mobility of each EV. The random variable V represents the vehicle velocity which has two possible values (i.e., a lower velocity v_L and a higher velocity v_H). The velocity transition is modeled as a two-state continuous-time Markov process with state transition rate $\frac{1}{D}$. Under this model, a vehicle initially chooses v_L (or v_H) and changes to v_H (or v_L) after an exponentially distributed time interval with mean D. The model can well describe the realistic human driving behaviors, that is, a driver tends to drive at a constant velocity for a period and then change to another velocity according to his/her will or road conditions. In addition, it is shown that when the vehicle density is low or medium (e.g., no larger than 30 vehicle/km/lane), vehicles can be considered to move independently [32], and that the headway distance[3] follows the exponential distribution with rate ζ [33].

When a mobile EV v ($\in \mathbb{V}$) is charged at Bus_j in period k, the charging load (denoted as $Pch_{v,j,k}$) should be within a certain range to protect the EV battery and power system stability, i.e.,

$$0 \leq Pch_{v,j,k} \leq Pch_{v,j,k}^{\max} \tag{3.4}$$

where $Pch_{v,j,k}^{\max}$ is the pre-fixed charging load upper bound of $Pch_{v,j,k}$ [34]. If EV v is not scheduled to be charged in period k, i.e., $x_{v,j,k} = 0$, $Pch_{v,j,k}$ should be 0, i.e.,

$$\frac{Pch_{v,j,k}}{Pch_{v,j,k}^{\max}} \leq x_{v,j,k} \tag{3.5}$$

[2] Note that if the distributed generation is adopted in the distribution system, the overloading problem should also be considered.

[3] In this chapter, the headway distance is defined as the distance between two neighboring vehicles in the same lane.

Meanwhile, $x_{v,j,k}$ should satisfy

$$\begin{aligned} &\sum_{j\in H} x_{v,j,k} \leq 1 \; and \; x_{v,j,k} \in X = [0,1] \cap \mathbb{Z} \\ &\sum_{k}\sum_{j\in H} x_{v,j,k} \leq X_{max} \end{aligned} \tag{3.6}$$

where X_{max} is the maximum total charging times for an EV within all the considered periods, since frequent charging is not desirable and may cause battery damages [35]. During a charging period, the charged energy of each EV should be limited by its battery capacity $C^{\max}_{battery}$, and the battery should not be depleted on the way to guarantee that the EV can be charged successfully, i.e.,

$$0 \leq P^{init}_{v,k} + (\sum_{j\in H} a \cdot Pch_{v,j,k} - P^{v,k}_{cost} - P^{k}_{cons} \cdot (1 - \sum_{j\in H} x_{v,j,k})) \leq C^{\max}_{battery} \tag{3.7}$$

where $P^{init}_{v,k}$ is the initial energy stored in EV v in the beginning of period k, which can be obtained through VANETs, and $P^{v,k}_{cost}$ is the travel cost for EV v to charge in period k. Notation P^{k}_{cons} denotes the average non-charging energy cost of each EV while moving on the road if the EV is not scheduled to charge in period k. The duration of each period is a hours. For example, if each period has a 30-min duration, $a = 0.5$. Then, for an EV charging station at Bus_j, the total EV charging load $Pch_{j,k}$ in period k is given as

$$Pch_{j,k} = \sum_{v\in\mathbb{V}} Pch_{v,j,k}. \tag{3.8}$$

3.2.4 Transmission Model in VANETs

To enable V2V and V2R transmissions in VANETs, we use the draft standard IEEE 802.11p [36] (DSRC), a standard designed particularly for short-range and intermittent vehicular communications among vehicles and RSUs. For analytical simplicity, ideal medium access control (MAC) protocol is considered. With the ideal MAC, the interference among V2V transmissions can be avoided; and as long as one vehicle moves into the coverage range of an RSU, the RSU is able to schedule time portions for V2R transmission between the vehicle and the RSU without collisions. In addition, we consider that a V2V or V2R link has a constant transmission rate, and the contact duration between each V2V or V2R transmission pair is long enough to complete one packet delivery. This could be achieved by properly setting the packet size [37–39]. Moreover, as the high mobility may make the vehicle communications to be intermittent, the waiting time to grab a transmission opportunity dominates the transmission delay over the queueing delay and the random backoff time introduced by the channel contention. Thus, in this chapter, we only consider the dominant delay part, i.e., the former one.

3.3 Problem Formulation

In this section, we first derive the charging load constraints for the buses connected with the EV charging stations, where the relation among the load capacities of the buses connected with the EV charging stations are unveiled. Then, considering the EV mobility, we formulate the EV's travel cost to represent the EV range anxieties. Particularly, the travel cost incurred by the transmission delay in VANETs is involved. Finally, we formulate the mobility-aware coordinated EV charging problem into an optimization problem, with the objective to maximize the overall charging-energy-minus-travel-cost while avoiding the power system overload. The objective jointly considers improving the total charging energy and reducing the charging travel cost. In other words, the total energy utilization and the travel cost for EV charging should be carefully balanced.

3.3.1 Charging Load Constraints

The charging station at Bus_j has a load-capacity constraint P^j_{total}, i.e., the total EV charging load at Bus_j in period k should be no more than P^j_{total}. Thus we have

$$Pch_{j,k} \leq P^j_{total}. \tag{3.9}$$

In addition, the voltage of one bus will decrease with the increased load [29]. If a voltage drops below a threshold at a bus, the reactive power cannot be properly and efficiently injected. To keep the voltage within a certain range, it is necessary to keep the load below a desired level. Therefore, tradeoff should exist between voltages and loads. In the following, we show the essential relation among the EV charging load capacities of buses in Theorem 3.1. The corresponding proof is given based on the power flow analysis in the power system.

Theorem 3.1 (Linear relation among EV charging loads of buses). *Given the total supplied power from the feeder and the non-EV charging load, the total power supply for all EV charging stations can be obtained. The power supplied for one individual charging station has a* linear relation *with that of the other charging stations.*

Proof. For each bus, the voltage should be no less than the minimal required voltage, e.g., 0.9 per unit voltage [9]. According to (3.3), the lowest voltage is $V_{N,k}$ of Bus_N. Then we have,

$$V_{N,k} = V_{1,k} - \sum_{i=1}^{N-1} [P_{i(i+1),k} \cdot r_{i(i+1)} + Q_{i(i+1),k} \cdot x_{i(i+1)}] \geq V_{min} \tag{3.10}$$

where V_{min} is the minimal required voltage. Re-arranging Eq. (3.10), we can get

$$\sum_{i=1}^{N-1} [P_{i(i+1),k} \cdot r_{i(i+1)} + Q_{i(i+1),k} \cdot x_{i(i+1)}] \leq V_{1,k} - V_{min}. \tag{3.11}$$

Let w denote the sorted index of the bus with no EV charging load and W the set of these buses $w \in W(\subset N)$. Denote the sorted index of the bus with EV charging load with j and the set of these buses as H, $j \in H(\subset N)$. Then, (3.11) can be expressed by

$$\sum_{w \in W} (P_{w(w+1),k} \cdot r_{w(w+1)} + Q_{w(w+1),k} \cdot x_{w(w+1)}) + \sum_{j \in H} j \cdot (P_{j,k} \cdot r_j + Q_{j,k} \cdot x_j) \leq V_{1,k} - V_{min} \tag{3.12}$$

where $P_{j,k}$ and $Q_{j,k}$ are the active and reactive power load on Bus_j in period k, respectively, and $r_j = \frac{1}{j} \sum_{h=1}^{j-1} r_{h(h+1)}$ and $x_j = \frac{1}{j} \sum_{h=1}^{j-1} x_{h(h+1)}$ denotes the average impedance of the feeder line between Bus_1 and Bus_j. Since the loads on the buses with no EV charging are known through the forecast, we have

$$\sum_{j \in H} j(P_{j,k} \cdot r_j + Q_{j,k} \cdot x_j) \leq V_{1,k} - V_{min} - \sum_{w \in W} (P_{w(w+1),k} \cdot r_{w(w+1)} + Q_{w(w+1),k} \cdot x_{w(w+1)}). \tag{3.13}$$

As each charging station is connected to the grid through a single-phase AC connection and EV charging only draws active power, we have $P_{j,k} = Pch_{j,k}$ and $Q_{j,k} = 0$. Thus, we can re-write (3.13) as

$$\sum_{j \in H} jPch_{j,k} \cdot r_j \leq \Xi \tag{3.14}$$

where Ξ is a constant representing the right hand side (RHS) of inequality (3.13). The inequality (3.14) indicates that the locations and the total number of the charging stations play important roles in the total available power supply to EV charging stations. Given the total power supply to EV charging stations, i.e., Ξ, the total load of the EV charging station at Bus_j in period k, $Pch_{j,k}$, presents a *linear relation* with the others. □

3.3.2 Travel Cost for EV Charging

According to Sect. 3.2.3, the travel cost for EV v to be charged in period k, $P_{cost}^{v,k}$, have two parts. The first part is the travel cost due to the travel distance from the EV v's current location to a charging station in period k, denoted as $p_{v,k}$. As mobile EVs may have different locations and battery levels at different periods. Due to the range anxiety, drivers tend to go to the closer charging stations with less travel distance. Thus the travel distance will affect the travel cost significantly.

The second part is the travel cost due to the transmission delay for EV v to receive a charging decision through VANETs, denoted as $c_{v,k}$. The vehicle mobility can cause intermittent transmission delay in VANETs. The resultant intermittent V2V and R2V connections can incur a transmission delay and thus involve an additional travel distance until EV v receives the charging decision from the RSUs or neighboring vehicles. Thus the transmission delay should also be considered when evaluating the travel cost.

1. *Travel cost due to the EV travel distance to a charging station*: If EV v is scheduled to be charged in the next period k, then $\sum_{j\in H} x_{v,j,k} = 1$. The shortest path algorithm [40] is exploited to calculate the traveling path for EV v to the charging station j in period k by the installed GPS. Denote the path length as $S(x_{v,j,k})$. Thus, the travel distance of EV v in period k for charging can be expressed as

$$p_{v,k} = \sum_{j\in H} S(x_{v,j,k}) \cdot x_{v,j,k}. \tag{3.15}$$

   Given $p_{v,k}$, define the travel cost in terms of energy of EV v in period k as $PC(p_{v,k})$. The notation $PC(\cdot)$ is a linear non-decreasing function that measures the impacts of travel distance on the travel cost [10].
2. *Travel cost due to the transmission delay in VANETs*: The second part of the travel cost is introduced by the transmission delay of an EV to send (or receive) the charging request (or decision) to (or from) the neighboring vehicle or nearest RSU.

We first derive the transmission delay of the last hop of the entire transmission path (i.e., the last V2R hop). The last-hop transmission delay mainly comes from the inter-contact time between a vehicle and an RSU. We model the last hop transmission into an "on-off" model [31]. Specifically, the vehicle either connects directly to an RSU during the "on" state or is the first vehicle approaching the RSU in front of which there is no other vehicles within the transmission range of the RSU in the "off" state. As the transmission delay for a packet in the "on" state is far smaller than that in the "off" state, the "off" period dominates the transmission delay. Both "on" and "off" periods are random variables and denoted as T_{on} and T_{off}, respectively. Accordingly, denote the travel distances within the periods as U_{on} and U_{off}, respectively, satisfying $T_{on} = \frac{U_{on}}{V}$ and $T_{off} = \frac{U_{off}}{V}$. The notation V is the average velocity of a vehicle based on the mobility model adopted in Sect. 3.2.3. Inspired by [31], the event that a vehicle moves a distance of at least u during T_{on} before being scheduled to transmit with RSU should satisfy two conditions: (1) no other vehicles are within the distance u from the considered vehicle, and (2) at least

another vehicle is within the distance $2R - u$ so that the considered vehicle has to move at least u distance to avoid the collision. Here, R is the transmission range of an RSU or a vehicle. Then, the probability that $U_{on} > u$ is calculated as

$$P_r(U_{on} > u) = \frac{(e^{-\zeta \cdot u})^{b\Gamma-1}[1-(e^{-\zeta \cdot (2R-u)})^{b\Gamma-1}]}{1-(e^{-\zeta \cdot 2R})^{b\Gamma}} \tag{3.16}$$

where b and Γ denote the total length of roads and the vehicle density on the roads, respectively. As aforementioned in Sect. 3.2.3, the vehicle headway distance follows an exponential distribution, thus, the probability that a headway distance is larger than u is $e^{-\zeta \cdot u}$. Thus the average U_{on} can be calculated as

$$E(U_{on}) = \int_0^{2R} P_r(U_{on} > u)du. \tag{3.17}$$

Similarly, the occurrence of the event that a vehicle moves a distance of at least u during the "off" period should satisfy that (1) no vehicles are within a $2R+u$ distance from the end of the coverage range of the nearest RSU ahead of the vehicle, and (2) there is at least one another vehicle within the distance $L - (u + 2R)$. Here, L is the distance between the adjacent RSUs. Then, the average travel distance during the "off" period can be calculated similarly as

$$P_r(U_{off} > u) = \frac{(e^{-\zeta \cdot (2R+u)})^{b\Gamma-1}[1-(e^{-\zeta \cdot (L-(2R+u))})^{b\Gamma-1}]}{(e^{-\zeta \cdot 2R})^{b\Gamma}[1-(e^{-\zeta \cdot (L-2R)})^{b\Gamma}]} \tag{3.18}$$

$$E(U_{off}) = \int_0^{L-2R} P_r(U_{off} > u)du. \tag{3.19}$$

As for the previous hops of the entire message transmission path, they are V2V communication links which can be characterized using the vehicle mobility model. The evolution process of the relative velocity between two adjacent vehicles can be modelled by a continuous time Markov chain (CTMC) with a state space $\mathbb{H} = \{h_0, h_1, h_2\}$. Here, h_0 denotes a negative relative velocity when the vehicle ahead moves with v_L while the vehicle behind moves with v_H; h_1 models a zero relative velocity when both vehicles move with the same speed; and h_2 denotes a positive relative velocity. If the period that each vehicle keeps the same velocity is exponentially distributed with the average value D, the transition rate between any two states of the CTMC is $2/D$. Thus, according to [31], the average number of hops M within the entire message transmission path can be estimated as

$$M = \frac{6(L-E[U_{on}]-E[U_{off}])}{D(v_L+v_H)}. \tag{3.20}$$

Based on Eq. (3.20), the transmission delay of the whole transmission path can be given as

$$\psi = (M-1)E[T_{V2V}] + E[T_{off}] \tag{3.21}$$

where $E[T_{V2V}]$ is the average transmission delay for a V2V hop satisfying that $E[T_{V2V}] = \frac{1}{1-e^{\zeta R}}$, since the headway distance follows an exponential distribution. If we consider the request sending and decision receiving as similar processes, the total transmission delay for a vehicle from sending the charging request to receiving the charging decision should be 2ψ. It can be seen that this transmission delay is dependent on the network parameters such as vehicle mobility parameters (i.e., v_L, v_H, ζ and D), the vehicle density (i.e., Γ), and the RSU deployment in the network (i.e., the transmission range R and the average inter-RSU distance L).

Therefore, the average travel distance, $c_{v,k}$, when EV v is moving and waiting for the charging decision in period k, can be obtained as

$$c_{v,k} = E[O_v] \cdot \sum_{j \in H} x_{v,j,k} \tag{3.22}$$

where $O_v = V \cdot 2\psi(v_L, v_H, D, \zeta, \Gamma, R, L)$ denotes the travel distance for EV v due to the transmission delay of VANETs. Similarly, the corresponding travel cost in terms of energy is defined as a linear non-decreasing function $PC(c_{v,k})$ to measure the energy cost consumed by EV v when waiting for the charging decision in period k.

With the defined $PC(p_{v,k})$ and $PC(c_{v,k})$, the initial stored energy, $P_{v,k}^{init}$, should be no less than the summation of $PC(p_{v,k})$ and $PC(c_{v,k})$ in order to guarantee the vehicle to reach the destination charging station, i.e.,

$$P_{cost}^{v,k} = PC(p_{v,k}) + PC(c_{v,k}) \leq P_{v,k}^{init}. \tag{3.23}$$

Note that $P_{v,k}^{init}$ can be collected in a real-time way by RSUs via VANETs.

3.3.3 Mobility-Aware EV Charging Optimization Problem

Have derived both the linear relationship among the load capacities of the charging stations and the travel cost for EVs, the charging strategy aims at maximizing the overall charged-energy-minus-travel-cost while avoiding power system overload [26]. The objective function indicates that improving the total charged energy and reducing the travel cost for EV charging will be jointly considered and deliberately balanced. Specifically, Upon receiving (1) the historic readings from the RTUs installed at the buses and (2) the vehicle information via VANETs, the traffic server conducts the charging strategy to determine $Pch_{v,j,k}$ and $x_{v,j,k}$, following the optimization problem below.

$$
\begin{aligned}
&\max \quad \sum_{k}\sum_{v\in\mathbb{V}}\sum_{j\in H} a\cdot Pch_{v,j,k} \; - \sum_{k}\sum_{v\in\mathbb{V}}(PC(p_{v,k})+PC(c_{v,k}))\\
&s.t.\\
&0 \le Pch_{v,j,k} \le Pch^{\max}_{v,j,k}, \forall v \in \mathbb{V}, \forall j \in H, \; and \; \forall k\\
&Pch_{j,k} = \textstyle\sum_{v\in\mathbb{V}} Pch_{v,j,k} \le P^{j}_{total}, \forall k, \forall j \in H\\
&\sum_{j\in H} jPch_{j,k}\cdot r_j \le \Xi, \; \forall k\\
&0 \le P^{init}_{v,k} + (\sum_{j\in H} a\cdot Pch_{v,j,k} - PC(p_{v,k}) - PC(c_{v,k}) - P^{k}_{cons}\cdot(1-\sum_{j\in H} x_{v,j,k}))\\
&\le C^{\max}_{battery}, \forall v \in \mathbb{V}, \forall k\\
&\frac{Pch_{v,j,k}}{Pch^{\max}_{v,j,k}} \le x_{v,j,k}, \forall v \in \mathbb{V}, \forall j \in H, \; and \; \forall k\\
&\sum_{j\in H} x_{v,j,k} \le 1 \; and \; x_{v,j,k} \in X = [0,1]\cap\mathbb{Z}, \forall v \in \mathbb{V}, \forall j \in H, \; and \; \forall k\\
&PC(p_{v,k}) + PC(c_{v,k}) \le P^{init}_{v,k}, \forall v \in \mathbb{V}, \forall k\\
&\sum_{k}\sum_{j\in H} x_{v,j,k} \le X_{max}, \forall v \in \mathbb{V}
\end{aligned}
\tag{3.24}
$$

With constraints given in (3.4), (3.7), (3.9), (3.14) and (3.23).

3.4 The Coordinated Mobility-Aware EV Charging Strategy

In this section, the solution of the optimization problem (3.24) is derived to obtain charging decisions. The original problem (3.24) is a time-coupled mixed-integer linear programming (MILP) problem, which is very complicated to solve. However, having noticed that there is only one time-coupled constraint, i.e., the last constraint of (3.24), the original time-coupled problem can be first time-decoupled into a set of sub-MILPs exploiting Lagrange duality [26]. The optimal solutions from all the sub-MILPs can be combined into an ϵ-optimal solution to the original problem [41]. That is, leveraging Lagrange duality, only solving each decoupled sub-MILP problem in each period can result in an ϵ-optimal solution for the whole time horizon. As for each sub-MILP, the optimal solution can be achieved by the branch-and-cut-based outer approximation (BCBOA) algorithm [27]. We also provide the proof for the optimality of BCBOA.

3.4.1 Optimization Decoupling Leveraging Lagrange Duality

By applying the Lagrange duality, the original optimization problem (3.24) is decoupled into a set of sub-problems w.r.t period k. The basic principle is to integrate the time-coupled constraints of (3.24) into the objective function by adding a weighted sum of the time-coupled constraints to the objective function. In this way, the original problem can be time-decoupled into a set of sub-problems w.r.t

period k, each only having decision variables and parameters of the same period. The essential philosophy underlying the feasibility of Lagrange duality for time-decoupling is that (i) the objective function is linear, and (ii) all the constrains are also linear [41]. We define the Lagrangian function $L(.)$ for the problem (3.24) as

$$L(Pch_{v,j,k}, x_{v,j,k}) = \sum_{k} \{\sum_{v\in\mathbb{V}} \sum_{j\in H} a \cdot Pch_{v,j,k} - \sum_{v\in\mathbb{V}} (PC(p_{v,k}) + PC(c_{v,k}))\} - \sum_{v\in\mathbb{V}} \iota_v [\sum_{k} \sum_{j\in H} x_{v,j,k} - X_{max}] \tag{3.25}$$

where ι_v represents the Lagrange multipliers corresponding to the vth inequality constraint

$$\sum_{k} \sum_{j\in H} x_{v,j,k} \leq X_{max}. \tag{3.26}$$

The vector $\{\iota_v\}$ is called the dual variable set or Lagrange multiplier vector. Rearranging Eq. (3.25), we can have

$$L(Pch_{v,j,k}, x_{v,j,k}) = \sum_{k} \{(\sum_{v\in\mathbb{V}} \sum_{j\in H} a \cdot Pch_{v,j,k}) - \sum_{v\in\mathbb{V}} (PC(p_{v,k}) + PC(c_{v,k})) - \sum_{v\in\mathbb{V}} \iota_v [\sum_{j\in H} x_{v,j,k}]\} + \sum_{v\in\mathbb{V}} \iota_v X_{max}. \tag{3.27}$$

The problem can then be decoupled into a set of isolated sub-problems w.r.t to each period k with the method of dual decomposition [26]. Denote with $D^k(\iota_v)$ the maximum value of Lagrangian $L(.)$ over $Pch_{v,j,k}$ and $x_{v,j,k}$ in period k, i.e.,

$$D^k(\iota_v) = \max_{Pch_{v,j,k}, x_{v,j,k}} \{(\sum_{v\in\mathbb{V}} \sum_{j\in H} a \cdot Pch_{v,j,k}) - \sum_{v\in\mathbb{V}} (PC(p_{v,k}) + PC(c_{v,k})) - \sum_{v\in\mathbb{V}} \iota_v [\sum_{j\in H} x_{v,j,k}]\}. \tag{3.28}$$

Then, define Lagrangian dual function $D(\iota_v)$ as the maximum of Lagrangian $L(.)$ over $Pch_{v,j,k}$ and $x_{v,j,k}$, and we have

$$D(\iota_v) = \sum_{k} D^k(\iota_v) + \sum_{v\in\mathbb{V}} \iota_v X_{max}. \tag{3.29}$$

By minimizing the Lagrangian dual function over the dual variables, ι_v, the ϵ-optimal solution of (3.24) can be achieved.

$$\begin{aligned} &\min_{\iota_v} D(\iota_v) \\ &\text{s.t.} \iota_v \geq 0. \end{aligned} \tag{3.30}$$

As proven in [41], given ι_v, if the solution $Pch_{v,j,k}$ and $x_{v,j,k}$ is optimal for problem (3.28) and satisfies the time-coupled constraint in (3.26), the solution is the ϵ-optimal to the original problem, with $\epsilon = -\sum_{v\in\mathbb{V}} \iota_v[\sum_k \sum_{j\in H} x_{v,j,k} - X_{max}]$.

3.4.2 Solving the Sub-MILP Problem Based on BCBOA Algorithm

According to (3.28), the sub-optimization problem, P, is given as

$$
P\begin{cases}
\max\limits_{Pch_{v,j,k}, x_{v,j,k}} \{(\sum\limits_{v\in\mathbb{V}}\sum\limits_{j\in H} a\cdot Pch_{v,j,k}) - \sum\limits_{v\in\mathbb{V}}(PC(p_{v,k}) + PC(c_{v,k})) - \sum\limits_{v\in\mathbb{V}} \iota_v[\sum\limits_{j\in H} x_{v,j,k}]\} \\
s.t. \\
f_{j,1}(x, Pch) = Pch_{j,k} = \sum_{v\in\mathbb{V}} Pch_{v,j,k} - P^j_{total} \le 0, \forall j \in H \\
f_2(x, Pch) = \sum\limits_{j\in H} Pch_{j,k}\cdot jr_j - \Xi \le 0 \\
f_{v,3}(x, Pch) = P^{init}_{v,k} + (\sum\limits_{j\in H} a\cdot Pch_{v,j,k} - PC(p_{v,k}) - PC(c_{v,k}) - P^k_{cons}(1 - \sum\limits_j x_{v,j,k})) - C^{\max}_{battery} \le 0, \\
\qquad\qquad \forall v \in \mathbb{V} \\
f_{v,4}(x, Pch) = -[P^{init}_{v,k} + (\sum\limits_{j\in H} a\cdot Pch_{v,j,k} - PC(p_{v,k}) - PC(c_{v,k}) - P^k_{cons}(1 - \sum\limits_j x_{v,j,k}))] \le 0, \forall v \in \mathbb{V} \\
f_{v,j,5}(x, Pch) = \frac{Pch_{v,j,k}}{Pch^{\max}_{v,j,k}} - x_{v,j,k} \le 0, \forall v \in \mathbb{V}, \forall j \in H \\
f_{v,6}(x, Pch) = \sum\limits_{j\in H} x_{v,j,k} - 1 \le 0, \forall v \in \mathbb{V} \\
f_{v,7}(x, Pch) = PC(p_{v,k}) + PC(c_{v,k}) - P^{init}_{v,k} \le 0, \forall v \in \mathbb{V} \\
0 \le Pch_{v,j,k} \le Pch^{\max}_{v,j,k}, \;\; x_{v,j,k} \in \{0,1\}, \;\; \forall v \in \mathbb{V}, \forall j \in H
\end{cases} \tag{3.31}
$$

where x and Pch are the set of all $x_{v,j,k}$ and $Pch_{v,j,k}$, respectively.

The sub-optimization problem (3.31) is an MILP, which can be solved by the BCBOA Algorithm [27]. The BCBOA algorithm is an iterative procedure which solves the original MILP by solving an alternating sequence of relaxed MILPs and linear programs (LPs). The relaxed MILP is achieved by replacing the original constraints with linear functions by means of polyhedral outer approximations (OAs). The OA is to provide polyhedral representation of the feasible space of P. The polyhedral representation renders linearly in the continuous variable, and enables complexity reduction for the original problem. Given any set of possible solutions $\mathbb{T} = \{(x^1, Pch^1), \ldots, (x^t, Pch^t), \ldots\}$, the MILP is given as follows,

$$
P^{OA}(T)\begin{cases}
\max \varpi \\
s.t. \\
\nabla G(x, Pch)^T_{|(x^t, Pch^t)} \begin{pmatrix} x - x^t \\ Pch - Pch^t \end{pmatrix} + G(x^t, Pch^t) \ge \varpi \\
\nabla F(x, Pch)^T_{|(x^t, Pch^t)} \begin{pmatrix} x - x^t \\ Pch - Pch^t \end{pmatrix} + F(x^t, Pch^t) \le 0 \\
\forall (x^t, Pch^t) \in \mathbb{T}, \; x \in X \cap Z^n, \; 0 \le Pch_{v,j,k} \le Pch^{\max}_{v,j,k}, \varpi \in R
\end{cases} \tag{3.32}
$$

where

$$G(x, Pch) = \{(\sum_{v\in\mathbb{V}}\sum_{j\in H} a \cdot Pch_{v,j,k}\ ) - \sum_{v\in\mathbb{V}} (PC(p_{v,k}) + PC(c_{v,k})) - \sum_{v\in\mathbb{V}} \iota_v[\sum_{j\in H} x_{v,j,k}]\},$$
$$F = \{f_{j,1}, f_2, f_{v,3}, f_{v,4}, f_{v,j,5}, f_{v,6}, f_{v,7}\},\ \forall v \in \mathbb{V},\ \forall j \in H,$$

ϖ is an auxiliary variable, and $\nabla G(\cdot)^T$ denotes the transpose of the gradient of G.

The LP can be achieved from the original problem P fixing x to $\bar{x}$, where $\bar{x}$ is the optimal solution of x in MILP (3.32). To summarize, the OA approximation exploits the gradients of both the objective and constraints at different points to build an MILP relaxation of the problem P. Note that as all the functions in problem P are linear, the relaxed MILP will be the same to the original problem in the first iteration, due to which the algorithm will terminate within two iterations at most. In the following, a proposed theorem shows that if (1) the solution set, $\mathbb{T}$, includes suitable points, and (2) KKT conditions are satisfied at these points, the problems $P^{OA}(T)$ and P are equivalent.

Theorem 3.2. *Consider that P has a finite set of optimal solutions. For* $\forall \bar{x} \in X \cap Z^n$, *if the problem*

$$P_{\bar{x}}\begin{cases} \max G(\bar{x}, Pch) \\ s.t. \\ f_{j,1} = \sum_{v\in\mathbb{V}} Pch_{v,j,k} - P^j_{total} \le 0,\ \forall j \in H \\ f_2 = \sum\limits_{j\in H} (Pch_{j,k} \cdot jr_j) = \sum\limits_{j\in H} (\sum\limits_{v\in\mathbb{V}} Pch_{v,j,k} \cdot jr_j) - \Xi \le 0 \\ f_{v,3} = P^{init}_{v,k} + (\sum\limits_{j\in H} a \cdot Pch_{v,j,k} - \overline{PC(p_{v,k})} - \overline{PC(c_{v,k})} - P^k_{cons}(1 - \sum\limits_j \overline{x_{v,j,k}})) - C^{\max}_{battery} \le 0, \forall v \in \mathbb{V} \\ f_{v,4} = -[P^{init}_{v,k} + (\sum\limits_{j\in H} a \cdot Pch_{v,j,k} - \overline{PC(p_{v,k})} - \overline{PC(c_{v,k})} - P^k_{cons}(1 - \sum\limits_j \overline{x_{v,j,k}}))] \le 0, \forall v \in \mathbb{V} \\ f_{v,j,5} = \frac{Pch_{v,j,k}}{Pch^{max}_{v,j,k}} - \overline{x_{v,j,k}} \le 0,\ \forall j \in H,\ \forall v \in \mathbb{V} \\ 0 \le Pch_{v,j,k} \le Pch^{\max}_{v,j,k} \end{cases} \tag{3.33}$$

is feasible, the optimal solution of $P_{\bar{x}}$, *denoted as* $\overline{Pch}$, *is optimal for P. Otherwise, if* $P_{\bar{x}}$ *is not feasible, the optimal solution to the following problem, also denoted as* $\overline{Pch}$, *is optimal to the problem P.*

$$P^F_{\bar{x}}\begin{cases} \min \sum\limits_{jj=1}^{|H|+1+2|\mathbb{V}|+|H||\mathbb{V}|} u_{jj} \\ s.t.\ \ f_{j,1} - u_{jj} \le 0,\ \ jj = \{1, \cdots, |H|\},\ j \in H \\ f_2 - u_{|H|+1} \le 0 \\ f_{v,3} - u_{jj} \le 0,\ \ jj = \{|H| + 2, \cdots, |H| + 1 + |\mathbb{V}|\},\ v \in \mathbb{V} \\ f_{v,4} - u_{jj} \le 0,\ \ jj = \{|H| + 2 + |\mathbb{V}|, \cdots, |H| + 1 + 2|\mathbb{V}|\},\ v \in \mathbb{V} \\ f_{v,j,5} - u_{jj} \le 0,\ \ jj = \{|H| + 2 + 2|\mathbb{V}|, \cdots, |H| + 1 + 2|V| + |\mathbb{V}||H|\},\ v \in \mathbb{V},\ j \in H \\ 0 \le Pch_{v,j,k} \le Pch^{\max}_{v,j,k} \end{cases} \tag{3.34}$$

where each u_{jj} *is one-to-one matched with each linear constraint (i.e.,* $f_{j,1}$, f_2, $f_{v,3}$, $f_{v,4}$, *and* $f_{v,j,5}$*), and there are totally* $|H| + 1 + 2|\mathbb{V}| + |H||\mathbb{V}|$ *constraints except the boundary constraints* $0 \le Pch_{v,j,k} \le Pch^{\max}_{v,j,k}$. *Define* $\bar{\mathbb{T}}$ *as the set of all such solutions*

$(\bar{x}, \overline{Pch})$. If the KKT conditions are satisfied at every point of $\bar{\mathbb{T}}$, P and $P^{OA}(\bar{\mathbb{T}})$ have the same optimal value.

Proof. Similar to [42], Denote the set of feasible $x \in X \cap Z^n$ in the problem $P_{\bar{x}}$ as X^F and the complement of X^F in $X \cap Z^n$ as X^I. Here, $X^F \neq \emptyset$.

When $\bar{x} \in X^I$, the problem $P_{\bar{x}}$ is infeasible and thus $\bar{\mathbb{T}}$ should contain the point $(\bar{x}, \overline{Pch})$ with an optimal solution of $P^F_{\bar{x}}$. Therefore, $P^{OA}(\bar{\mathbb{T}})$ contains the constraint

$$\begin{aligned} &\nabla F(x, Pch)^T_{|(\bar{x},\overline{Pch})} \begin{pmatrix} x - \bar{x} \\ Pch - \overline{Pch} \end{pmatrix} + F(\bar{x}, \overline{Pch}) \leq 0 \\ &where\ F = \{f_{j,1}, f_2, f_{v,3}, f_{v,4}, f_{vj,5}, f_{v,6}, f_{v,7}\},\ \forall v \in \mathbb{V},\ \forall j \in H. \end{aligned} \tag{3.35}$$

Moreover, as $\overline{Pch}$ is an optimal solution of $P^F_{\bar{x}}$ and the KKT conditions are satisfied, there exists $\mu \in R_+^{2*[|H|+1+2|\mathbb{V}|+|H||\mathbb{V}||]}$ such that the first $|H| + 1 + 2|\mathbb{V}| + |\mathbb{V}| \cdot |H|$ elements in μ has one-to-one mapping with each constraint in F and

$$\begin{aligned} &\sum_{jj=1}^{|H|+1+2|\mathbb{V}|+|H||\mathbb{V}|} \mu_{jj} \nabla_{Pch}[f_{jj}(\bar{x}, \overline{Pch})] = 0,\ \ \forall f_{jj} \in \\ &F = \{f_{j,1}, f_2, f_{v,3}, f_{v,4}, f_{vj,5}\},\ \forall v \in \mathbb{V},\ \forall j \in H. \end{aligned} \tag{3.36}$$

$$1 - \mu_{jj} - \mu_{|H|+1+2|\mathbb{V}|+|\mathbb{V}|\cdot|H|+jj} = 0,\ \ jj = 1, \ldots, |H| + 1 + 2|\mathbb{V}| + |\mathbb{V}| \cdot |H| \tag{3.37}$$

$$\mu_{jj}[f_{jj}(\bar{x}, \overline{Pch}) - \bar{u}_{jj}] = 0,\ \ jj = 1, \ldots, |H| + 1 + 2|\mathbb{V}| + |\mathbb{V}||H| \tag{3.38}$$

$$\mu_{|H|+1+2|\mathbb{V}|+|\mathbb{V}||H|+jj} \bar{u}_{jj} = 0,\ \ jj = 1, \ldots, |H| + 1 + 2|\mathbb{V}| + |\mathbb{V}||H|. \tag{3.39}$$

According to (3.35), it can be further derived that

$$\nabla_{Pch}[f_{jj}(\bar{x}, \overline{Pch})]^T \left(Pch - \overline{Pch}\right) + f_{jj}(\bar{x}, \overline{Pch}) \leq 0, jj = 1, \cdots, |H| + 1 + 2|\mathbb{V}| + |H||\mathbb{V}|, \forall f_{jj} \in F. \tag{3.40}$$

Add $|H| + 1 + 2|\mathbb{V}| + |H||\mathbb{V}|$ inequalities in (3.40) with the nonnegative multipliers $\mu_1, \ldots, \mu_{|H|+1+2|\mathbb{V}|+|H|\cdot|\mathbb{V}|}$. After rearranging, it can be obtained that

$$\sum_{j=1}^{|H|+1+2|\mathbb{V}|+|H||\mathbb{V}|} \mu_{jj} \nabla_{Pch}[f_{jj}(\bar{x}, \overline{Pch})]^T (Pch - \overline{Pch}) \leq - \sum_{j=1}^{|H|+1+2|\mathbb{V}|+|H||\mathbb{V}|} \mu_{jj} f_{jj}(\bar{x}, \overline{Pch}),\ \forall f_{jj} \in F. \tag{3.41}$$

According to (3.36), the left hand side (LHS) of (3.41) equals to zero. While according to (3.38), the RHS of (3.41) equals to $- \sum_{jj=1}^{|H|+1+2|\mathbb{V}|+|H||\mathbb{V}|} \mu_{jj} \bar{u}_{jj}$. From (3.39), $\mu_{jj+|H|+1+2|\mathbb{V}|+|\mathbb{V}||H|} = 0$ if $\overline{u_{jj}} > 0,\ \forall jj \in \{1, \ldots, |H| + 1 + 2|\mathbb{V}| + |\mathbb{V}||H|\}$. Then, combining (3.37), we have $\mu_{jj} = 1$ for $\forall jj \in \{1, \ldots, |H| + 1 + 2|\mathbb{V}| + |\mathbb{V}||H|\}$ satisfying $\overline{u_{jj}} > 0$. This implies that the RHS of (3.41), i.e., $- \sum_{jj=1}^{|H|+1+2|\mathbb{V}|+|\mathbb{V}||H|} \bar{u}_{jj}$,

is strictly negative otherwise $P_{\bar{x}}$ would be feasible. Therefore, the inequality (3.41) has no solution, which indicates that the maximum value of $P^{OA}(\bar{\mathbb{T}})$ is to be found as the maximum value over all $x \in X^F$.

In addition, let $\overline{Pch}$ be an optimal solution to $P_{\bar{x}}$. $(G(\bar{x}, \overline{Pch}), \bar{x}, \overline{Pch})$ is a feasible solution of $P^{OA}_{\bar{x}}(\bar{\mathbb{T}})$. Thus, $G(\bar{x}, \overline{Pch})$ is a lower bound on the optimal value ϖ of $P^{OA}_{\bar{x}}(\bar{\mathbb{T}})$. In the following, the value $G(\bar{x}, \overline{Pch})$ is proved to be also an upper bound, i.e., $\varpi \leq G(\bar{x}, \overline{Pch})$. When $\overline{Pch}$ is an optimal solution of $P_{\bar{x}}$ and satisfies the KKT conditions. There exists $\mu \in \mathbb{R}_+^{|H|+1+2|\mathbb{V}|+|\mathbb{V}||H|}$ such that

$$-\nabla_{Pch} G(\bar{x}, \overline{Pch}) + \sum_{jj=1}^{|H|+1+2|\mathbb{V}|+|\mathbb{V}||H|} \mu_{jj} \nabla_{Pch}[f_{jj}(\bar{x}, \overline{Pch})] = 0, \ \forall f_{jj} \in F \tag{3.42}$$

$$\mu_{jj} f_{jj}(\bar{x}, \overline{Pch}) = 0, \ jj = 1, \ldots, |H| + 1 + 2|\mathbb{V}| + |\mathbb{V}||H|. \tag{3.43}$$

With outer-approximation programming, any solution of $P^{OA}_{\bar{x}}(\bar{\mathbb{T}})$ should satisfy

$$\begin{aligned} &-\nabla_{Pch} G(\bar{x}, \overline{Pch})^T \left(Pch - \overline{Pch}\right) - G(\bar{x}, \overline{Pch}) \leq -\varpi \\ &\nabla_{Pch}[f_{jj}(\bar{x}, \overline{Pch})]^T (Pch - \overline{Pch}) + f_{jj}(\bar{x}, \overline{Pch}) \leq 0, \ \ jj = 1, \cdots, |H| + 1 + 2|\mathbb{V}| + |\mathbb{V}||H| \end{aligned} \tag{3.44}$$

Multiply the second inequality set in (3.44) by the Lagrange multipliers (i.e., $\mu_{jj} \geq 0$) and subsequently add to the first inequality in (3.44). Then, re-arrange the LHS and we can obtain

$$\begin{aligned} &\{-\nabla_{Pch} G(\bar{x}, \overline{Pch}) + \sum_{j=1}^{|H|+1+2|\mathbb{V}|+|\mathbb{V}||H|} \mu_{jj} \nabla_{Pch} f_{jj}(\bar{x}, \overline{Pch})\}^T \cdot \left(Pch - \overline{Pch}\right) \\ &+ \sum_{j=1}^{|H|+1+2|\mathbb{V}|+|\mathbb{V}||H|} \mu_{jj} f_{jj}(\bar{x}, \overline{Pch}) - G(\bar{x}, \overline{Pch}) = -G(\bar{x}, \overline{Pch}) \leq -\varpi. \end{aligned} \tag{3.45}$$

From (3.42) and (3.43), the LHS of (3.45) is equivalent to $-G(\bar{x}, \overline{Pch})$. Therefore, we have $G(\bar{x}, \overline{Pch}) \geq \varpi$; that is, for $\forall \bar{x} \in X^F$, the problem $P^{OA}_{\bar{x}}(\bar{\mathbb{T}})$ and $P_{\bar{x}}$ have the same optimal objective value. □

As given above, the optimality of BCBOA is proved. To summarize, the formulated optimal charging problem can be solved by first time-decoupling the original problem into a set of sub-MILPs through Lagrange duality, and each sub-MILP can be solved with the branch-and-cut-based outer approximation (BCBOA) algorithm. The charging decisions in terms of $Pch_{v,j,k}$ and $x_{v,j,k}$ can be dispatched to the involved EV via VANETs.

3.5 Performance Evaluation

We study a realistic suburban scenario shown in Fig. 3.4 – a region around the campus of University of Waterloo (Waterloo, ON, Canada). RSUs are uniformly deployed along roads. For the smart grid parameters, we use the parameters of the 12-bus distribution system (only load buses) provided in [29], with enlarging the load to MW level. Two charging stations are deployed as marked in Fig. 3.4a and connected to Bus_2 and Bus_{11}, respectively. Table 3.1 shows the load data at each bus at 21:00. We set the input voltage to 1.0 pu, and the minimum allowable voltage to 0.9 pu. The impedance of any line section is set to $0.005 + j0.0046$. Table 3.2 shows the normalized non-EV-charging power load over that at 21:00 for all the buses, according to the trend given in [43]. Vehicles move on the roads in the considered region following the mobility model in Sect. 3.2.3. To emulate the vehicle traffic, we employ a highly realistic microscopic vehicle traffic simulator, VISSIM [28], to generate vehicle trace files for recording the vehicle mobility information. Based on the trace files, the average transmission delay incurred by VANETs for an EV

Fig. 3.4 The simulation scenario of University of Waterloo region in VISSIM. (**a**) A snap shot of the simulation region with signing the simulated roads in *blue*. (**b**) The 3D vehicle traffic illustrations of two intersections highlighted in *red* on the upside

Table 3.1 An example of active and reactive power value at each bus of the system

Hour	Bus number	2	3	4	5	6	7	8	9	10	11	12
21:00	P(MW)	TBD	4.0	5.5	–	6.0	5.5	4.5	–	3.5	TBD	3.0
	Q(MVar)	–	3.0	5.5	–	1.5	5.5	4.5	–	3.0	–	1.5

Table 3.2 Normalized power over the power at 21:00 for all the buses without EV charging load during a day

Hour	1:00	2:00	3:00	4:00	5:00	6:00	7:00	8:00	9:00	10:00	11:00	12:00
Normalized power	0.5	0.5	0.5	0.5	0.7	0.9	1.3	1.5	2.1	2.3	2.5	2.5
Hour	13:00	14:00	15:00	16:00	17:00	18:00	19:00	20:00	21:00	22:00	23:00	24:00
Normalized power	2.5	2.3	2.1	1.8	1.5	1.4	1.3	1.2	1.0	0.7	0.7	0.7

to receive a charging decision is first evaluated. Then, combining with the power system data, the performance of the proposed mobility-aware EV charging strategy is investigated, leveraging a customized simulator built in Matlab. The proposed strategy is compared to an existing coordinated charging strategy that doe not consider the EV mobility or the travel cost [9]. The investigated performance metrics include the total EV charging energy (TECE), the average EV travel cost (AETC), and the percentage of EVs that succeed or fail in charging.

3.5.1 Simulation Setup

To simulate a VANET in VISSIM, in the initial stage of the simulation, vehicles are pushed into the region with area of 6000×2800 m as shown in Fig. 3.4a. Vehicles enter the region from the pre-set entries (nine entries at the ends of the main roads), following a Poisson arrival process with rate ζ (e.g., $\zeta = 2500$ vehicle/hour/entry). After a certain warm-up duration t_ζ (e.g., 240 s), the vehicle push-in stops and vehicle density will reach 30 vehicles/km/lane. The vehicle information (e.g., locations, velocities, etc.) is recorded at the end of each simulation step (e.g., 0.2 s) in the vehicle trace files. Besides, RSUs (e.g., 25 RSUs) are uniformly deployed along the roads in the considered region. The transmission range of both RSUs and vehicles is R (e.g., 150 m). The simulation lasts for 3000 s.

As for the car following model, we adopt the Wiedemann 74 model [44] for modeling the traffic. In this model, the vehicle acceleration is a function of the vehicle velocity, the driving behaviors of the driver, the features of the vehicle as well as the difference in distance and velocity between the subject vehicle and the vehicle in front [44]. At an intersection, the traffic is controlled by either the traffic lights or a stop sign, which is consistent with the reality, as illustrated in Fig. 3.4b.

All the vehicles follow the two-state random velocity model described in Sect. 3.2.3 with parameters $V = \{v_L, v_H\}$ and D (e.g., $v_L = 30$ km/h, $v_H = 60$ km/h, $D = 60$ s).

For the EV charging setup, the EV battery capacity is set to 85KWh according to the TESLA Model S [3]. The charging period is 30 min, during which a maximum of 30KWh energy can be charged. If an EV will not be charged in a period, the energy consumption for maintaining mobility in that period follows a uniform distribution over the interval [0,10] KWh. In addition, the maximal charging times for one EV (i.e., X_{max}) is set to be 3. For better illustration purpose, an existing centralized charging strategy proposed in [9] is compared which aims to only maximize the total amount of EV charging energy.

3.5.2 Simulation Results of VANETs

We first examine the validity of the mobility model proposed in Sect. 3.2.3 and the analytical results of (3.18) derived based on the mobility model, as shown in Fig. 3.5. Based on the trace files obtained from VISSIM, the probability density function (PDF) of vehicle headway distance is shown in Fig. 3.5a when $\zeta = 2500$ vehicles/hour/entry. It can be seen that the PDF of the headway distance matches well with an exponential distribution, which verifies the hypothesis in Sect. 3.2.3 that the headway distance will be exponentially distributed at low or medium vehicle density. In addition, the average headway distance can be calculated from the approximated exponential distribution in Fig. 3.5a, which is about 30 m. This average value is very close to that calculated from the pre-set vehicle density in simulation setup, i.e., 30 vehicles/km/lane. Furthermore, Fig. 3.5b validates the analytical PDF of the distance between the last hop vehicle to the nearest RSU for one packet delivery. With 25 RSUs deployed in the network, the theoretical PDF is calculated based on Eq. (3.18). The simulation results are extracted from the real trace files of VISSIM. It can be observed from Fig. 3.5b that the analytical PDF matches well with the simulated PDF, thus validating the efficacy of the analytical results in Eq. (3.18). Calculating from the simulation results, the average distance from the last hop vehicle to its neatest RSU is around 200 m.

Figure 3.5c presents the PDF of the headway distance when the vehicle density ζ decreases to 1800 vehicles/hour/entry. The PDF curve approximately follows an exponential distribution as well. The average distance is increased to 46 m. In addition, Fig. 3.5d illustrates the PDF of the last-hop V2R distance, from which the average V2R distance of the last hop is calculated to be about 215 m. This average V2R distance is also very close to the analytical results in Eq. (3.18).

We then show the single-hop connection probability between a vehicle and its nearest RSU and the end-to-end multi-hop transmission delay in VANETs, as shown in Figs. 3.6 and 3.7, respectively. The simulation is conducted with different RSU deployments (i.e., 25 or 8 RSUs in the network) and different vehicle densities (i.e., $\zeta = 2500$ or 1800 vehicles/hour/entry). From Fig. 3.6, it can be seen that when both the number of RSUs and ζ are fixed, the single-hop connection probability increases

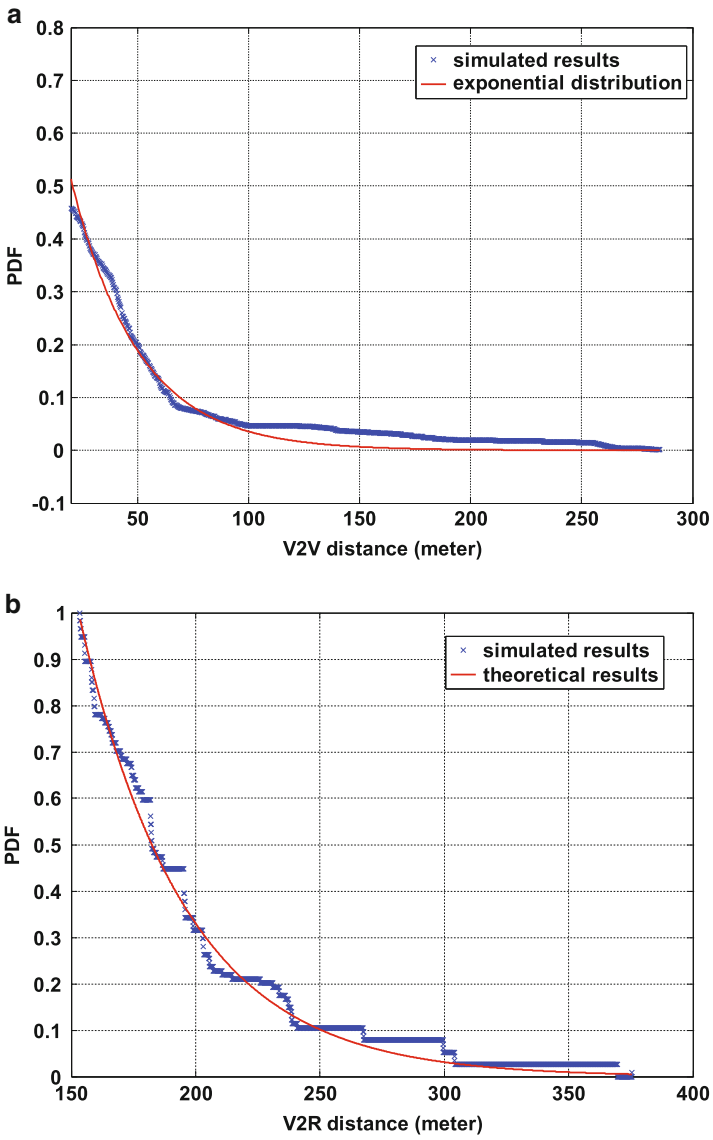

Fig. 3.5 (continued)

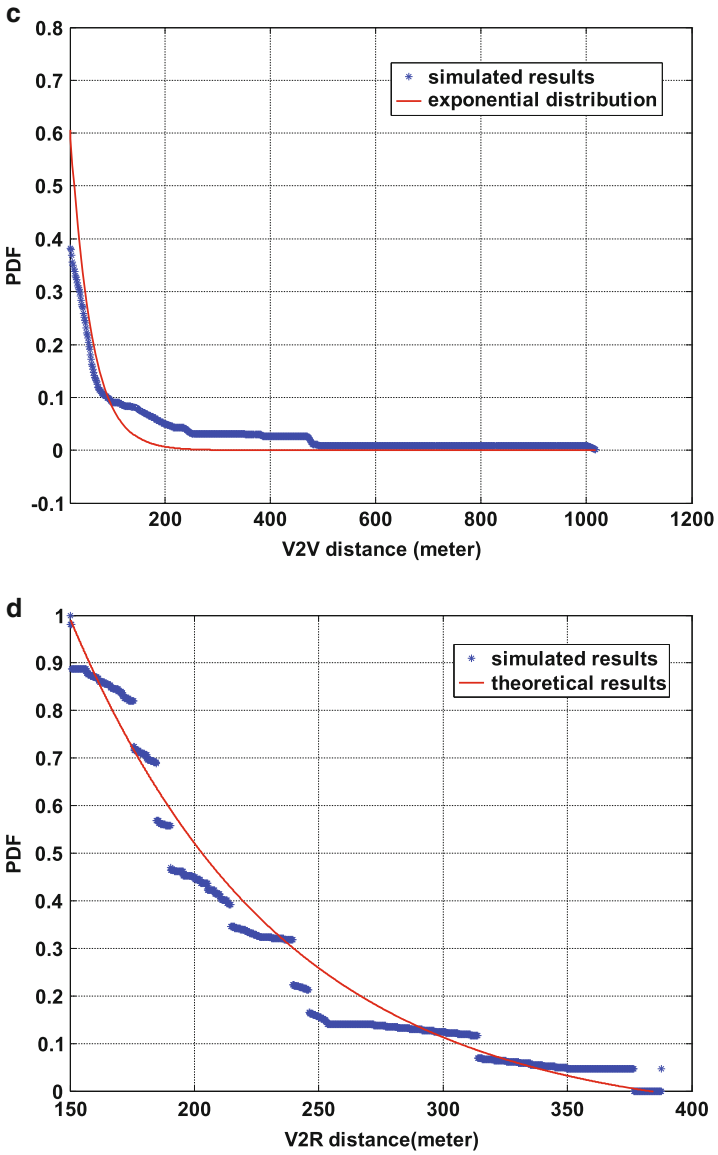

Fig. 3.5 The PDFs of both two adjacent vehicle distance (V2V distance) and the last hop V2R distance. (**a**) The PDF of V2V distance when $\zeta = 2500$. (**b**) The PDF of the last hop V2R distance when $\zeta = 2500$. (**c**) The PDF of V2V distance when $\zeta = 1800$. (**d**) The PDF of the last hop V2R distance when $\zeta = 1800$

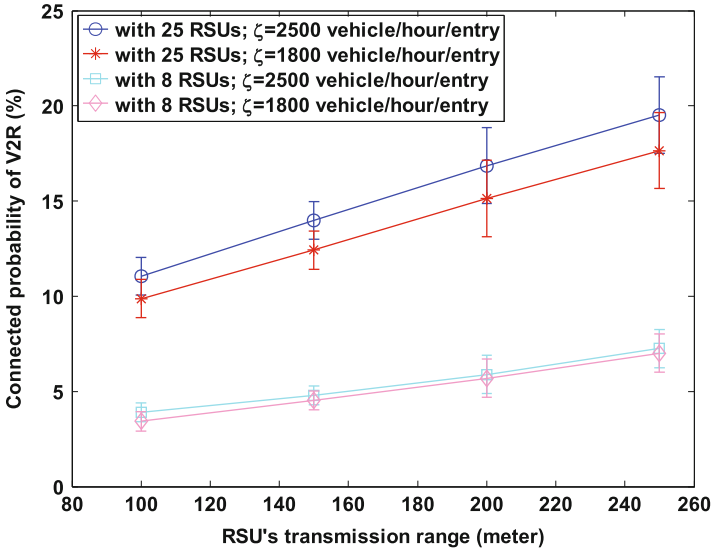

Fig. 3.6 The average connection probability between a vehicle and an RSU

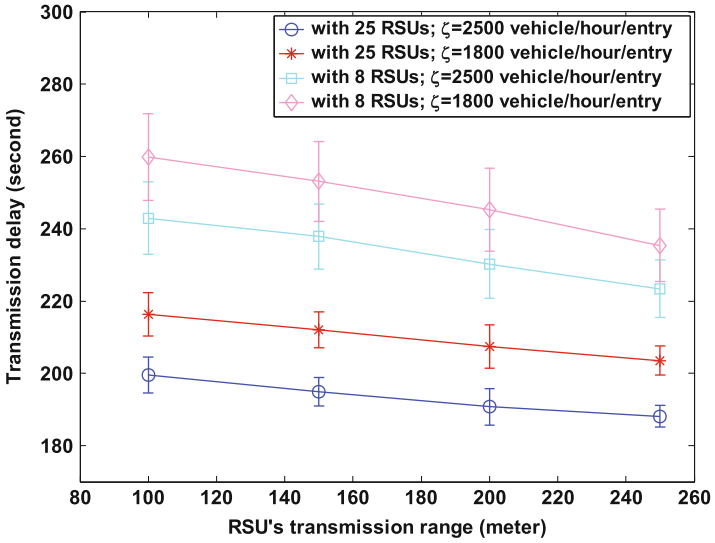

Fig. 3.7 The average transmission delay for a V2R uplink

as the RSU transmission range increases. In addition, when the RSU transmission range is fixed, the single-hop connection probability increases with more RSUs or larger ζ but to different extents; that is, the change in the number of RSUs impacts more on the connection probability than that in ζ. This is due to the following reasons. On one hand, as explained in the transmission model in Sect. 3.2.4, the transmission collisions could be avoided once vehicles are within the RSU coverage. Thus, the increase of ζ can only affect the connection probability via reducing the average U_{off}, as indicated in Eq. (3.18). On the other hand, the average headway distances when $\zeta = 2500$ and $\zeta = 1800$ are around 30 and 50, respectively, which are quite small compared to the RSU transmission range R. Thus, the two headway distances can be considered to be in the same scaling order. Consequently, the average U_{off} will not change a lot with the two simulated ζ values, so the gaps between the connection probabilities are very small when the RSU deployment is fixed. Contrarily, when ζ is fixed, different numbers of RSUs can lead to bigger difference in terms of the average U_{off}, resulting in a much larger gap.

From Fig. 3.7, it can be found that the average end-to-end transmission delay decreases with larger RSU transmission range, more deployed RSUs or larger ζ. A more interesting observation is that different from the single-hop connection probabilities, the end-to-end transmission delay does not increment a lot even when the number of RSUs largely decreases, e.g., from 25 to 8. For instance, the transmission delay is around 190 s when there are 25 RSUs and $\zeta = 2500$, and is around 240 s when there are 8 RSUs and $\zeta = 1800$. The small difference compared with the big gap of connection probability is attributed to the benefits brought by multi-hop V2V relaying. When there are much less deployed RSUs, although the single-hop connection probability (i.e., direct connection opportunity) from a vehicle to an RSU is significantly reduced, the multi-hop V2V transmission can still efficiently convey the information to an RSU at the cost of a small delay increase. In this way, the multi-hop V2V relaying increases the equivalent transmission range of a vehicle. In addition, with the considered parameter values, the average end-to-end transmission delay is around 200 s. This indicates that although the transmission delay of VANETs is larger than the cellular systems (e.g., LTE systems), it is still acceptable for the applications of vehicle information gathering compared with the decision making period (i.e., 30 min). More essentially, VANETs can significantly cut down the service expenses and boost the transmission rates, which matter more to large-volume vehicle data transmissions.

3.5.3 Simulation Results of the Proposed Charging Strategy

In this subsection, the performance of the proposed charging strategy is investigated. One thing to notice is that although the strategy is performed every 30 min, the simulation results are collected every 1 h. The TECE performance under a weekday total-available-charging-energy (TACE) profile [43] is first presented in Fig. 3.8. The profile figures are given in Table 3.2. The total number of EVs is fixed. Since

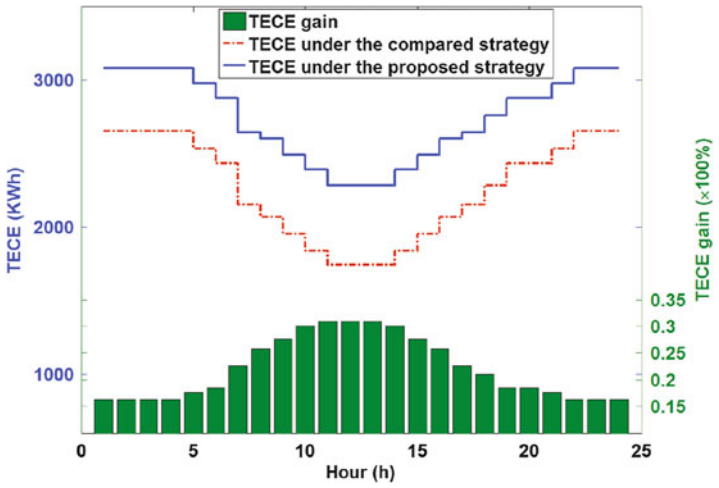

Fig. 3.8 Daily TECE comparison when the total number of EVs is fixed to 1200

our main focus is to study the performance of the charging strategies when the overload is likely to occur, only the case when the TACE is not sufficient to charge all the requesting EVs in each period is considered. From Fig. 3.8, tt can be seen that the proposed strategy can achieve larger TECE than the compared strategy in all the hours. The reason is as follows. In the compared strategy, no real-time vehicle information is considered, thus, the charging decisions are made without considering the EV mobility, range anxiety and the travel cost. Consequently, some EVs are likely to be scheduled to a charging station which is beyond reach based on their current locations and battery levels, because their batteries will be depleted on the way. Contrarily, our proposed strategy accounts for the travel cost derived from the real-time vehicle information from VANETs and only dispatches the EVs to the charging stations within their reach, thus leading to a larger TECE. In addition, the TECE gain ranges between 15 % and 30 % for different hours, and is larger when TACE is smaller. This is because when the TACE is smaller, there are more EVs that cannot be charged in the current period. Since the EVs are moving on the roads, they will continue to consume energy even if they are not charged. In consequence, there is less stored battery energy in the beginning of the next period, leading to a larger depletion probability if an EV is scheduled to a farther station under the compared strategy. Unlike the compared strategy, our strategy can effectively avoid the EV depletion, thus having a larger gain with smaller TACE.

We then examine the AETC performance under different TACE values in Fig. 3.9. It can be observed that the AETC under the proposed strategy is considerably smaller than that under the compared strategy, and the gain is larger when the TACE is larger. This is because the proposed strategy pays attention to reducing the AETC, thus tending to assign closer charging stations to EVs. With larger TACE, each charging station can charge more EVs at a time. Consequently, more EVs can be scheduled to the closer charging stations under the proposed strategy, resulting in a larger gain than the compared strategy.

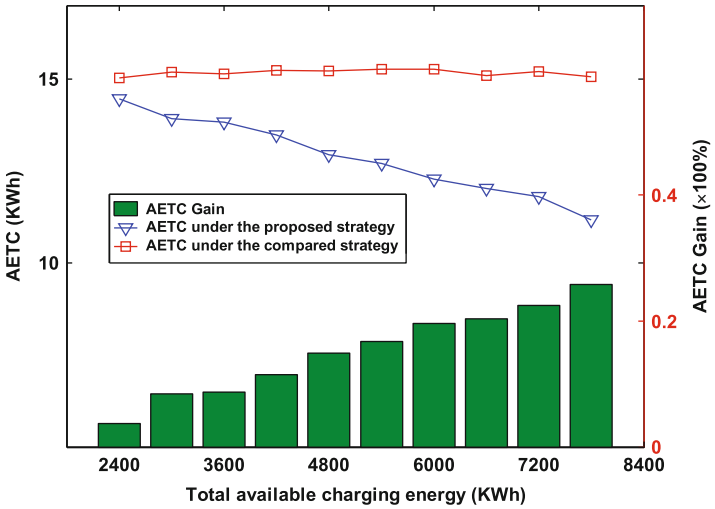

Fig. 3.9 AETC comparison with increasing TACE when the total number of EVs is 1200

Furthermore, the number of EVs that succeed or fail in charging under different strategies is compared in Fig. 3.10. It can be found that the proposed strategy has less involved EVs, which is the number of successfully charged EVs plus the number of EVs that fail to be charged, but more successfully charged EVs. This phenomenon further supports the explanation for Fig. 3.8. Since the proposed strategy tend to assign the EVs to the closer stations, the EV charging load is less balanced than the compared strategy. Thus, there are less involved EVs under the proposed strategy. However, the compared strategy may cause battery depletion for some involved EVs on their way, the EVs that actually succeed in charging are less than the proposed strategy. Therefore, it is crucial to take EV mobility and range anxiety into the charging strategy design for EV fast-charging context.

Last, the comparison of the AETC performance as well as the number of successfully charged EVs is shown in Fig. 3.11. It can be seen that with fixed TACE and increased total number of EVs, the AETC under the proposed strategy decreases, and there are more successfully charged EVs; while both metrics remain almost unchanged under the compared strategy. This is because the proposed strategy considers to reduce the AETC. When there are totally more EVs, more EVs that are closer to the charging stations get the charging opportunity. As a result, the AETC decreases correspondingly. When the AETC decreases, the scheduled EVs reach the charging stations with higher average battery levels, leading to a smaller average EV charging energy. Thus more EVs can be accommodated by the charging stations given that the TACE is fixed. But the compared strategy does not consider the AETC, the increase in the total number of EVs has little impact on the EV selection, thus resulting in almost unchanged performance.

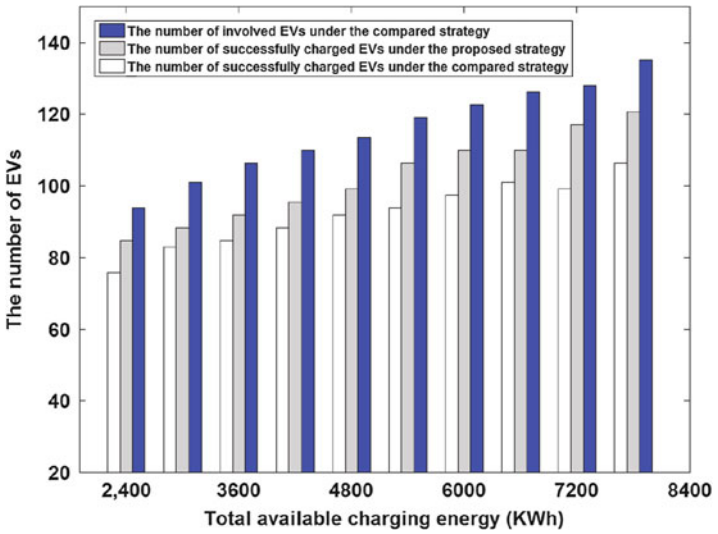

Fig. 3.10 Comparison of the number of involved EVs and successfully charged EVs, with 1200 EVs

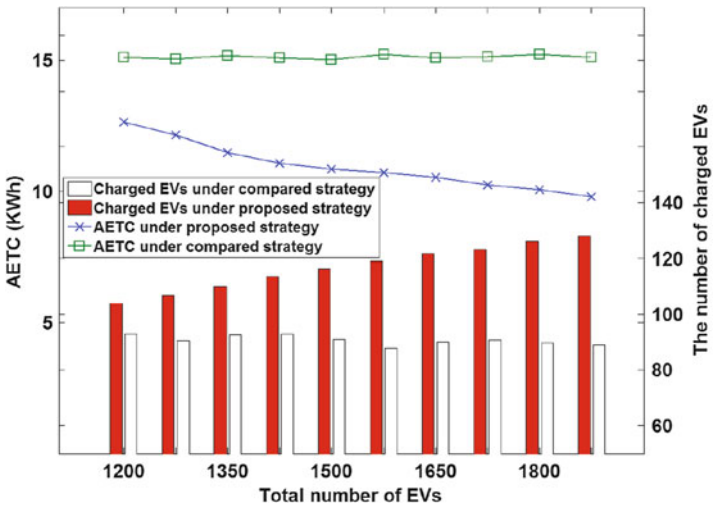

Fig. 3.11 Comparison of AETC and the number of successfully charged EVs, with fixed TACE (5400 KWh)

3.6 Related Work

Many studies [13, 14] have shown that high EV penetration levels can significantly affect the stability of the power system. To prevent the power system from overloading during the peak time, it is crucial to conduct load management strategies to distribute the EV charging load over both time and space [15]. In [9, 16], to evite power system overloading, some peak load is shaved and shifted to off-peak periods to improve the energy utilization for the entire grid. In [17, 18], it is shown that based on the global load information, the EV charging strategies that coordinate the charging duration and power rates of a group of EVs can have better performance than the local strategy. In [19, 20], the spatial diversity of EV charging is investigated to further help regulate the charging profile. Most of the existing EV charging strategies assume EVs to be stationary when they need to be charged. Few works take into account the vehicle mobility, which is the most distinct feature of a vehicle. The vehicle mobility can not be overlooked especially in fast-charging context. Due to vehicle mobility, the range anxiety, i.e., the tension between the travel cost and the EV battery level, is key to the feasibility of the charging decisions. Therefore, it is desirable to design new efficient EV charging strategies that incorporate the real-time vehicle information into solving the range anxiety problem.

To collect the real-time vehicle information, most existing works count on cellular or Wi-Fi systems [45–47]. However, the practicability in collecting the vehicle information is limited by inevitable drawbacks of these systems. First, for dense vehicle scenarios, the locational inaccuracy of both systems [48] may considerably degrade the charging performance. Second, as cellular systems are not used exclusively for vehicular communications, the vehicular services can be highly costly, and other cellular services may be congested by the high volume of vehicular data transmission especially under high the vehicle density; the coverage of the Wi-Fi systems is quite limited which may cause large latency for information delivery, and the delivery ratio may be dramatically reduced due to the high vehicle mobility. With VANETs, the transmission of the real-time messages can be much faster, cheaper and more efficient than the above systems, especially in a dense and highly mobile vehicular environment [37]. Dedicated to information exchange among highly mobile vehicles and the RSUs, short-range V2V and V2R communications are supported to effectively extend the transmission range of vehicles in a multi-hop manner and with higher data rates. The wired inter-RSU information sharing and various V2V relaying mechanisms can provide higher throughput and delivery ratio as well as lower latency for the large-volume vehicle information exchange [38, 39]. All these features make it possible to perform coordinated charging strategy for a group of vehicles. In this chapter, VANETs are integrated into a smart grid to enable the real-time information exchange among mobile vehicles and RSUs, and evaluate the end-to-end transmission delay incurred by VANETs. Then, the range anxiety is introduced as a viability indicator for the EV charging decisions.

Leveraging the real-time vehicle information collection and decision dissemination through VANETs, we aim at designing a mobility-aware coordinated predictive charging strategy for mobile EVs. The strategy enhances the energy utilization of the whole power system and reduces the average EV travel cost while preventing the power system from overloading. Our preliminary work [1] has investigated this subject, but does not consider the spatial diversity of charging stations and the additional transmission cost brought by the transmission delay in VANETs. Extending that work, this chapter incorporates charging location diversity and transmission delay into the optimization framework, and fully evaluates the impacts of these factors in a highly realistic suburban scenario built in VISSIM.

3.7 Conclusions

In this chapter, we have considered the EV mobility into the EV charging management and proposed a mobility-aware coordinated EV charging strategy to enhance the energy utilization and reduce the EV travel cost while avoiding the overload in power system. Specifically, a VANET-enhanced smart grid has been proposed with the capabilities to collect real-time vehicle information through VANETs. A predictive mobility-aware coordinated EV charging strategy has been put forward aiming to maximize the overall charging-energy-minus-travel-cost with overload avoidance. Extensive simulations have been conducted to evaluate the impacts of the transmission performance in VANETs on the EV charging performance and demonstrate that the proposed EV charging strategy can achieve considerably higher total charged energy, lower average EV travel cost and more successfully charged EVs than the existing strategy that does not consider the EV mobility and travel cost. In our future work, we intend to study the incentive mechanisms to stimulate the EVs to follow the charging decisions in order to achieve global optimality.

References

1. M. Wang, H. Liang, R. Deng, R. Zhang, X. Shen, VANET based online charging strategy for electric vehicles, in *Proceedings of the IEEE GLOBECOM'13*, Atlanta, Dec 2013
2. M. Wang, H. Liang, R. Zhang, R. Deng, X. Shen, Mobility-aware coordinated charging for electric vehicles in VANET-enhanced smart grid. IEEE J. Sel. Areas Commun. **32**(7), 1–17 (2014)
3. TESLA Motors, [Online] available: http://www.teslamotors.com/Pages/goelectric#
4. A comprehensive guide to plug-in hybrid vehicles, hybrid cars (2011), [Online] available: http://www.hybridcars.com/plug-in-hybrid-cars/$#$battery
5. Electric Power Resech Institute, [Online] available: http://www.epri.com/Pages/Default.aspx
6. A. Heider, H.J. Haubrich, Impact of wide-scale EV charging on the power supply network, in *IEEE Colloquium on Electric Vehicles – A Technology Roadmap for the Future*, London, vol. 6, no. 262, 1998, pp. 1–4

7. K. Nyns, E. Haesen, J. Driesen, The impact of charging plug-in hybrid electric vehicles on a residential distribution grid. IEEE Trans. Power Syst. **25**(1), 371–380 (2010)
8. I.S. Bayram, G. Michailidis, M. Devetsikiotis, F. Granelli, Electric power allocation in a network of fast charging stations. IEEE J. Sel. Areas Commun.: Smart Grid Commun. Ser. **31**(7), 1235–1246 (2013)
9. P. Richardson, D. Flynn, A. Keane, Local versus centralized charging strategies for electric vehicles in low voltage distribution systems. IEEE Trans. Smart Grid **3**(2), 1020–1028 (2012)
10. H. Liang, B.J. Choi, W. Zhuang, X. Shen, Optimizing the energy delivery via V2G systems based on stochastic inventory theory. IEEE Trans. Smart Grid **4**(4), 2230–2243 (2013)
11. P. Richardson, D. Flynn, A. Keane, Optimal charging of electric vehicles in low voltage distribution systems. IEEE Trans. Power Syst. **27**(1), 268–279 (2012)
12. J. Lopes, S. Polenz, C. Moreira, R. Cherkaoui, Identification of control and management strategies for LV unbalanced microgrids with plugged-in electric vehicles. IEEE J. Electr. Power Syst. Res. **80**(8), 898–906 (2010)
13. M. Shaaban, Y. Atwa, E. El-Saadany, PEVs modeling and impacts mitigation in distribution networks. IEEE Trans. Power Syst. **28**(2), 1122–1131 (2013)
14. D. Ban, G. Michailidis, M. Devetsikiotis, Demand response control for PHEV charging stations by dynamic price adjustments, in *Proceedings of the IEEE Innovative Smart Grid Technologies*, Washington, DC, Jan 2012
15. R.C. Green, L. Wang, M. Alam, The impact of plug-in hybrid electric vehicles on distribution networks: a review and outlook. J. Renew. Sustain. Energy Rev. **15**(1), 544–553 (2011)
16. G.T. Heydt, The impact of electric vehicle deployment on load management strategies. IEEE Trans. Power Appar. Syst. **1**(144), 1253–1259 (1983)
17. K. Mets, T. Verschueren, W. Haerick, C. Develder, F. Turck, Optimizing smart energy control strategies for plug-in hybrid electric vehicle charging, in *Proceedings of the IEEE Network Operations and Management Symposium Workshops*, Osaka, Apr 2010
18. K. Clement, E. Haesen, J. Driesen, Coordinated charging of multiple plug-in hybrid electric vehicles in residential distribution grids, in *Proceedings of the IEEE Power Systems Conference and Exposition*, Seattle, Mar 2009
19. L. Kelly, Probabilistic modeling of plug-in hybrid electric vehicle impacts on distribution networks in British Columbia, M. S. thesis, Department of Mechanical Engineering, University of Victoria, Victoria, 2009
20. S. Bae, A. Kwasinski, Spatial and temporal model of electric vehicle charging demand. IEEE Trans. Smart Grid **3**(1), 394–403 (2012)
21. H. Liang, W. Zhuang, Efficient on-demand data service delivery to high-speed trains in cellular/infostation integrated networks. IEEE J. Sel. Areas Commun. **30**(4), 780–791 (2012)
22. H. Liang, W. Zhuang, Double-loop receiver-initiated MAC for cooperative data dissemination via roadside WLANs. IEEE Trans. Commun. **60**(9), 2644–2656 (2012)
23. T.H. Luan, X. Shen, F. Bai, Integrity-oriented content transmission in the vehicular ad hoc networks, in *Proceedings of the IEEE INFOCOM*, Turin, Apr 2013
24. H.T. Cheng, H. Shan, W. Zhuang, Infotainment and road safety service support in vehicular networking: from a communication perspective. Mech. Syst. Signal Process. Spec. Issue Integr. Veh. Dyn. **25**(6), 2020–2038 (2011)
25. T.H. Luan, X. Ling, X. Shen, Provisioning QoS controlled media access in vehicular to infrastructure communications. IEEE Ad Hoc Netw. **10**(2), 231–242 (2012)
26. S. Boyd, L. Vandenberghe, *Convex Optimization* (Cambridge University Press, Cambridge, 2004)
27. M. Duran, I. Grossmann, An outer-approximation algorithm for a class of mixed-integer nonlinear programs. Math. Program. **36**(3), 307–339 (1986)
28. http://vision-traffic.ptvgroup.com/en-uk/products/ptv-vissim/
29. M.E. Elkhatb, R. El-Shatshat, M. Salama, Novel coordinated voltage control for smart distribution network with DG. IEEE Trans. Smart Grid **2**(4), 598–605 (2011)

30. L. Cheng, B.E. Henty, D.D. Stancil, F. Bai, P. Mudalige, Mobile vehicle-to-vehicle narrow-band channel measurement and characterization of the 5.9 GHz dedicated short range communication (DSRC) frequency band. IEEE J. Sel. Areas Commun. **25**(8), 1501–1516 (2007)
31. A. Abdrabou, W. Zhuang, Probabilistic delay control and road side unit placement for vehicular ad hoc networks with disrupted connectivity. IEEE J. Sel. Areas Commun. **29**(1), 129–139 (2011)
32. A. May, *Traffic Flow Fundamentals* (Prentice Hall, Englewood Cliffs, 1990)
33. N. Wisitpongphan, F. Bai, P. Mudalige, V. Sadekar, O. Tonguz, Routing in sparse vehicular ad hoc networks. IEEE J. Sel. Areas Commun. **25**(8), 1538–1556 (2007)
34. O. Hafez, Some aspects of microgrid planning and optimal distribution operation in the presence of electric vehicles, M. S. thesis, Department of Electrical and Computer Engineering, University of Waterloo, Waterloo, 2011
35. R. Nelson, Power requirements for batteries in hybrid electric vehicles. IEEE J. Power Source **91**(1), 2–26 (2000)
36. IEEE WG, *IEEE 802.11p/D2.01, Draft Amendement to Part 11: Wireless Medium Access Control (MAC) and Physical Layer (PHY) specifications: Wireless Access in Vehicular Environments*, Mar 2007
37. N. Lu, N. Zhang, N. Cheng, X. Shen, J. Mark, F. Bai, Vehicles meet infrastructure: toward capacity-cost tradeoffs for vehicular access networks. IEEE Trans. Intell. Transp. Syst. **14**(3), 1266–1277 (2013)
38. M. Wang, H. Shan, L.X. Cai, N. Lu, X. Shen, F. Bai, Throughput capacity of VANETs by exploiting mobility diversity, in *Proceedings of the IEEE ICC'12*, Ottawa, June 2012
39. N. Lu, T. Luan, M.Wang, X. Shen, F. Bai, Bounds of asymptotic performance limits of social proximity vehicular networks. IEEE/ACM Trans. Netw. **22**(3), 812–825 (2014)
40. M. Abboud, L. Jaoude, Z. Kerbage, Real time GPS navigation system (2004), http://webfea-lb.fea.aub.edu.lb/proceedings/2004/SRC-ECE-27.pdf
41. A. Geoffrion, Lagrangean relaxation for integer programming. Math. Program. Study **2**, 82–114 (1974)
42. P. Bonami, L. Biegler, A. Conn, G. Cornuejols, I. Grossmann, C. Laird, J. Lee, A. Lodi, F. Margot, N. Sawaya, A. Wachter, An algorithmic framework for convex mixed integer nonlinear programs. J. Discret. Optim. **5**(2), 186–204 (2008)
43. C. Norén, J. Pyrko, Typical load shapes for Swedish schools and hotels. Energy Build. **28**(2), 145–157 (1998)
44. R. Wiedemann, Modeling of RTI-elements on multi-lane roads, in *Proceedings of the Drive Conference*, Brussels, Feb 1991
45. J. Herrera, D. Work, R. Herring, X. Ban, A. Bayen, Evaluation of traffic data obtained via GPS-enabled mobile phones: the mobility century field experiment. Working Paper UCB-ITS-VWP-2009-8, Aug 2009
46. R. Herring, A. Hofleitner, S. Amin, Using mobile phones to forecast arterial traffic through statistical learning, in *Proceedings of the 89th Annual Meeting of Transportation Research Board*, Washington, DC, Jan 2010
47. K. Lee, J. Lee, Y. Yi, I. Rhee, S. Chong, Mobile data offloading: how much can wifi deliver? in *Proceedings of the ACM Co-NEXT*, New York, Nov 2010
48. H. Liu, A. Danczyk, R. Brewer, R. Starr, Evaluation of cell phone traffic data in Minnesota. Transp. Res. Rec. **2086**(1), 1–7 (2008)

Chapter 4
Coordinated V2V Fast Charging for Mobile GEVs Based on Price Control

Vehicle-to-vehicle (V2V) charging strategies offer charging plans for gridable electric vehicles (GEVs), targeting at offloading the GEV charging loads from the electric power systems. However, designing an effective and efficient online V2V charging strategy with optimal energy utilization remains an open issue. In this chapter, a price control based semi-distributed online V2V charging strategy is put forward for an energy swapping station. Specifically, through electricity price control, GEVs are stimulated to participate in V2V energy transactions by offering high revenues for the discharging GEVs and low cost for the charging GEVs. The Oligopoly game theory and Lagrange duality optimization techniques are leveraged to solve the formulated optimal V2V charging problems. Simulation are conducted to demonstrate the performance of the proposed V2V charging strategy.

4.1 Introduction

Electric vehicles (EVs) have attracted ever-increasing interest worldwide as an important diagram for sustainable and eco-friendly transportation systems. Partly (or fully) refueled with electricity, EVs provide great potentials to save huge costs for drivers during the vehicle lifetime. For example, a TESLA Model S, which is a pioneering retail battery EV produced by TESLA Motors, costs $3,492 for 100,000 miles, while a conventional gasoline-powered premium sedan costs $17,727 for the same distance [1]. Besides, the EVs solely powered by electricity generate no emissions (e.g., greenhouse gas emissions), thus reducing pollution to the environment. However, overload problems due to EV charging may be caused by the high penetration of EVs, which is even prominent when fast EV charging is considered as much higher power is required than the that in regular charging.

In most of the common EV charging strategies, EVs draw energy from the power grid via charging stations, referred to as grid-to-vehicle (G2V). However, when the

M. Wang et al., *Mobile Electric Vehicles*, Wireless Networks,
DOI 10.1007/978-3-319-25130-1_4

EV charging demand is high, overload situation may become a threat for the power grid, leading to power supply failure. Thus, it is indispensable to design an efficient and economical EV charging framework to relieve the overload problem. Thanks to the installed bi-directional chargers in EVs, the EVs not only draw the energy from the power grid with G2V plug-in functionalities but also inject energy back to the grid, referred to as discharging via vehicle-to-grid (V2G). We also refer to the EVs with bi-directional chargers as gridable EVs (GEVs) [2]. Thus, the bi-directional interaction between PEVs and the grid enables the vehicle-to-vehicle (V2V) charging, where energy can be directly transferred from one group of GEVs to another group of GEVs at an aggregator (e.g., energy swapping stations) [2]. In this way, the heavy EV charging load can be offloaded from the power grid for the purpose of overload avoidance. With V2V, the efficiency for GEV charging can be significantly improved, i.e., the requirements of infrastructure can be simplified and the power loss can be lowered.

To the best of our knowledge, there has been little emphasis put to investigate the charging/discharging coordination strategies in a context of V2V charging. The primary distinct feature of a V2V strategy from the conventional charging strategies is that, in addition to coordinating charging for a set of charging GEVs, another set of GEVs need to be stimulated to discharge the energy such that the demand can be matched with the supply. In this chapter, a semi-distributed price control based GEV charging strategy is proposed at a swapping station connected to the power grid in a V2V scenario. In specific, under the electricity price control strategy, GEVs are stimulated to participate in a V2V energy transaction where high revenue and low cost are anticipated for discharging GEVs and charging GEVs, respectively. Moreover, the proposed strategy targets the mobile GEVs (e.g., electric taxis), and thus has to consider the range anxiety in the problem formulation. The range anxiety refers to the tension between the GEV travel cost[1] and the energy levels of the batteries equipped with the GEVs. We model the discharging procedure into a single-period Oligopoly game with one product [3], i.e., the GEVs with surplus energy will compete to decide the electricity price and the amount of individual discharging power in the stage of price decision making, aiming to maximize their own revenues. Based on this determined price, the demanding GEV charging problem is formulated into a convex optimization problem with the objective to minimize the overall charging costs.

4.2 System Model

The proposed V2V strategy is able to perform online coordination for GEV charging and discharging. Thus, real-time information exchange is needed among vehicles and between vehicles and the swapping station. The realtime information includes

[1] In this chapter, the GEV energy consumed on the road to reach a swapping station is referred to as the travel cost.

price control related signalings and (dis)charging decisions. The heterogeneous wireless network infrastructure proposed in [4] is adopted, where the cellular networks and vehicular ad-hoc networks (VANETs) are combined to collect and disseminate information in a real-time manner.

Large coverage can be provided by the cellular networks via a set of base stations (BSs), however, the service cost can be high and congestion may be caused for other cellular services [5]. On the contrary, VANETs enable short-range communications between vehicles and road side units (RSUs) (i.e., V2R communications) and among vehicles (i.e., V2V communications[2]), which is realized via deploying much cheaper RSUs along the road side and installing on-board communication facilities (e.g., on-board units (OBUs)) in the vehicles. But due to the short single-hop coverage, VANETs suffer from intermittent connections among vehicles and RSUs. Therefore, by combining both networks, the resultant heterogeneous wireless network can make full use of the advantages of both networks while remedying their limitations.

In this section, a heterogeneous wireless network-enhanced V2V charing architecture is first introduced. Then, the GEV mobility and charging/discharging models are presented. At last, the price control model for the V2V charging strategy is discussed.

4.2.1 Heterogeneous Wireless Network-Enhanced V2V Charging

As shown in Fig. 4.1, the proposed heterogeneous wireless network-enhanced V2V charing architecture is composed of a swapping station, the GEVs, RSUs along the road side, and a BS of the cellular network.

The swapping station is an aggregator for V2V fast charging/discharging among GEVs. No energy is stored in the swapping station, which is only responsible for determining electricity prices for charging/discharging via supply-demand matching. The time horizon is slotted into periods, each with duration τ. In the beginning of every period, based on the collected GEV charging/discharging profiles, electricity price is determined at the swapping station for the following period.

RSUs are distributed along the roads with the capability of collecting the GEV (dis)charging information (i.e., charging and discharging profiles of GEVs) through V2V relaying and V2R transmissions. In addition, the cellular network also supports the wireless connections between the BS and portable transceivers in GEVs. Moreover, RSUs and BSs have wireline connections with the swapping station, thus being able to forward the collected charging/discharging profiles to the

[2]Note that, in this chapter, the term V2V is used in two different contexts, one for VANET communications among vehicles and the other for energy transfer among EVs.

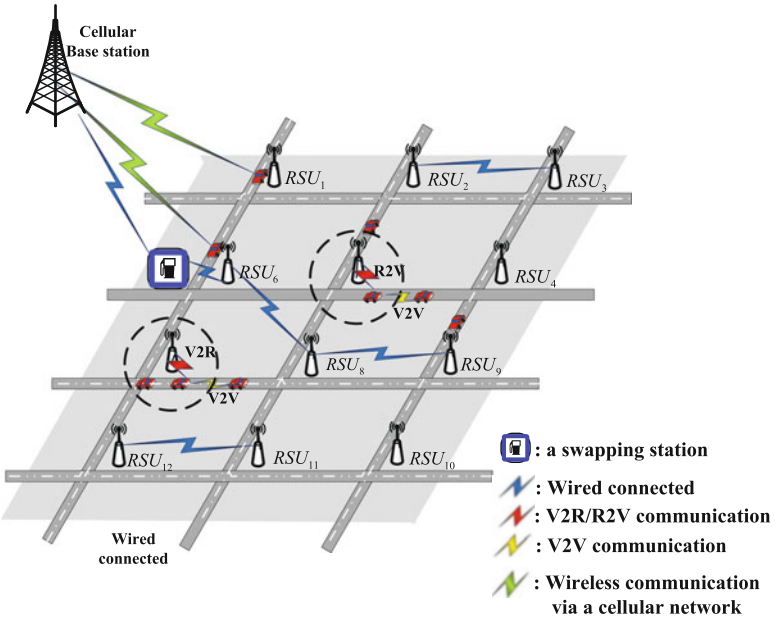

Fig. 4.1 V2V charing architecture

swapping station for price decision. Once any RSU/BS obtains the price control decisions from the swapping station, it can relay the price to GEVs via short-range high-speed R2V and V2V communications or long-range low speed cellular communications.

Denote the set of mobile GEVs as $\mathbb{V}$. GEVs may decide to (dis)charge when moving on the roads, e.g., electric taxis. All GEVs are considered with the same battery capacity, denoted as C. Each GEV is equipped with both network interfaces for cellular network and VANETs. Both profile information collection and price dissemination can be accomplished either through multi-hop V2V and V2R transmissions or directly via the BS communications. Based on the received price control information, the discharging decisions are made through competition among GEVs; the charging decisions are made aiming to minimize the overall costs. The range anxiety of each GEV is considered in both decision procedures. The charging/discharging decision of GEV v is the charging/discharging load/rate at the swapping station in period k, which can be denoted as $P_{v,k}$. After that, the GEV (dis)charging decisions are sent back to swapping stations via the heterogeneous wireless network.

The set of candidate GEVs with surplus energy thus able to discharge is denoted as $\mathbb{S} \in \mathbb{V}$, and the set of candidate GEVs with charging demands is denoted as $\mathbb{D} \in \mathbb{V}$. For GEV d ($d \in \mathbb{D}$) with charging demand, the charging load is denoted as $P_{d,k}$; similarly, for GEV s ($s \in \mathbb{S}$) with surplus energy, the discharging load is denoted as $P_{s,k}$.

4.2.2 GEV Mobility Model

The adopted mobility model for each GEV depicts vehicle mobility by two variables (V, J) [6], where V is a random variable representing the vehicle velocity and has two possible values (i.e., a lower velocity v_L and a higher velocity v_H). The notation J is the average time for a vehicle staying in either velocity state.

4.2.3 GEV (Dis)Charging Models

4.2.3.1 GEV Charging Models

If a mobile GEV is charged in one period, the charging load of GEV d ($\in \mathbb{D}$) in period k, i.e., $P_{d,k}$, should be within a certain range constrained by the GEV charger output power, that is,

$$0 \leq P_{d,k} \leq P_{d,k}^{\max} \tag{4.1}$$

where $P_{d,k}^{\max}$ is the pre-set discharging load upper bound for $P_{d,k}$ [7]. Then, the sum load of GEVs that need charging in period k, denoted as P_D^k, can be given as

$$P_D^k = \sum_{d \in \mathbb{D}} P_{d,k} \tag{4.2}$$

4.2.3.2 GEV Discharging Models

For discharging GEVs, the discharging power $P_{s,k}$ is upper-bounded by the pre-set value $P_{s,k}^{\max}$ due to the charger power constraint [8],

$$0 \leq P_{s,k} \leq P_{s,k}^{\max} \tag{4.3}$$

Then, the total discharged energy from GEVs in period k at the swapping station, which is denoted as P_S^k, is

$$P_S^k = \sum_{s \in \mathbb{S}} P_{s,k} \tag{4.4}$$

4.2.4 Electricity Price Model

Figure 4.2 illustrates the functionality framework for the price control based semi-distributed V2V charging strategy. Based on the collected information on GEV charging demand and discharging capabilities (i.e., approximated maximum power

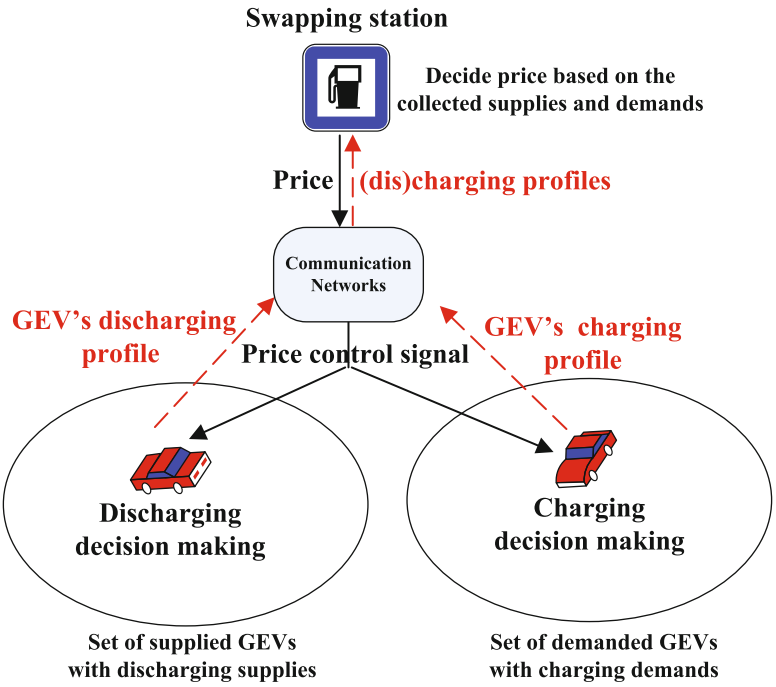

Fig. 4.2 An illustration of semi-distributed V2V (dis)charging strategy based on price control

demand $\mathbb{P}_{\mathbb{D}}$ and power supply $\mathbb{P}_{\mathbb{S}}$), the swapping station determines the electricity price u. There are two cases when deciding the price as follows.

- High demand case: If $\mathbb{P}_{\mathbb{D}} > \mathbb{P}_{\mathbb{S}}$, the electricity price is determined by the supply side, i.e., $u = a - bP_S^k$, where a and b are positive coefficients of the linear price function [9]. In this case, some GEVs that need charging may not be charged, i.e., $P_{d,k} = 0$ for some GEVs, in order to match the demand with the supply at the swapping station. This case will be explained in details in the next section.
- Surplus supply case: If $\mathbb{P}_{\mathbb{S}} \geq \mathbb{P}_{\mathbb{D}}$, the electricity price is determined by the demand side, i.e., $u = a - bP_D^k$. In this case, some GEVs with surplus energy may not contribute to the V2V transaction (due to low revenue and excessive potential energy supply), i.e., $P_{s,k} = 0$ for some GEVs, again, in order to satisfy the supply and demand matching at the swapping station, which will be explained in the next section.

After electricity price is fixed, a price control message is disseminated to GEVs via the heterogeneous wireless communication network. Based on the price, GEVs will make their charging/discharging decisions to either minimize the charging cost or maximize the discharging revenue, with considering their range anxieties. Note

that in the first stage, price is derived at the swapping station in a centralized manner; while the charging/discharging decisions are made at individual GEVs in a distributed way. Thus, our strategy is a semi-distributed one.

4.3 Problem Formulation

In this section, we first present the power balance constraint at the swapping station and the charging/discharging load constraints for GEVs. Then, the travel costs of GEVs are defined and formulated.

4.3.1 Balance Constraint at the Swapping Station

In order to realize charging/discharging control for GEVs, the power balance constraint at the swapping station need to be first discussed. In a V2V transaction, the power balance equation is the basic power constraint among GEV chargers. The physical meaning of the power balance equation is that at the swapping station, the total charged power should be equal to the total discharged power. I.e., for the discharging GEVs (i.e., $s \in \mathbb{S}$) and charging GEVs (i.e., $d \in \mathbb{D}$) in period k, we have

$$\sum_{s \in \mathbb{S}} \eta_s P_{s,k} = \sum_{d \in \mathbb{D}} \eta_d P_{d,k}. \tag{4.5}$$

where $\eta_s \in (0, 1]$ ($\eta_d \in (0, 1]$) is the discharging (charging) efficiency of the charger for all the GEV suppliers (demanders) [2].

4.3.2 GEV Charging Constraints

During a charging period, the charged energy of each GEV is limited by its battery-capacity (denoted as C), and the battery should not be depleted on the way to the swapping station, i.e.,

$$0 \leq E_{d,k}^{init} + (a \cdot \eta_d P_{d,k} - P_{cost}^{d,k}) \leq C, \quad \forall d \in \mathbb{D} \tag{4.6}$$

where $E_{d,k}^{init}$ denotes the initial battery level of GEV d in period k, and $P_{cost}^{d,k}$ denotes the travel cost of GEV d for charging in period k (to be detailed in Sect. 4.3.4). The duration of each period is a hours. For example, if the charging duration for each period is 15 min, $a = 0.25$. The charging duration is considered to be the same for

all the GEVs. Denote the charging cost for GEV d as $c_{d,k}$. With charging load $P_{d,k}$ in period k, $c_{d,k}$ can be expressed as

$$c_{d,k} = u_k \cdot (a \cdot \eta_d P_{d,k} + P_{cost}^{d,k}) \tag{4.7}$$

where u_k denotes the energy price, as determined by the swapping station.

4.3.3 GEV Discharging Constraints

The discharged energy of each discharging GEV is also limited by its battery capacity C, and the battery should not be depleted on the way for discharging. After the discharging, GEV s need to keep a minimum amount of energy C_s in its battery to ensure its capability to complete its own journey after period k. Thus, we have

$$C_s \leq E_{s,k}^{init} + (-a\eta_s P_{s,k} - P_{cost}^{s,k}) \leq C, \quad \forall s \in \mathbb{S} \tag{4.8}$$

where $E_{s,k}^{init}$ denotes the initial battery level in GEV s in period k. Notation $P_{cost}^{s,k}$ denotes the travel cost for discharging in period k for GEV s (to be detailed in Sect. 4.3.4). The discharging cost for GEV s in period k is denoted as $c_{s,k}$. With the discharged power $P_{s,k}$, there are three components for $c_{s,k}$, which are travel cost, energy discharging cost, and battery wear cost, respectively, i.e.,

$$c_{s,k} = u_s \cdot (a \cdot \eta_s P_{s,k} + P_{cost}^{s,k}) + W_s \tag{4.9}$$

where u_s is the price at which GEV s purchased its stored energy. The notation $W_s = e_1(a\eta_s P_{s,k})^2 + e_2(a\eta_s P_{s,k}) + e_3$ represents the quadratic battery wear cost function for GEV s [8], where e_1, e_2, and e_3 are non-negative coefficients. Thus, the revenue $R_{s,k}$ of GEV s can be calculated as

$$R_{s,k} = u_k \cdot a\eta_s P_{s,k} - c_{s,k}. \tag{4.10}$$

4.3.4 Travel Cost for (Dis)Charging GEV

The travel cost $P_{cost}^{v,k}$ for GEV v to be charged/discharged in period k is composed of two parts. First, as GEVs are moving, they may have different locations at different periods, one part of the travel cost is related to the travel distance from the GEV's current location to the swapping station. Second, the travel cost is also related to the transmission delay of the heterogeneous wireless network since GEV v is still moving while waiting for the required price information from the swapping station. According to the mobility model described in Sect. 3.2.3, the transmission delay is in a much finer time scale (say seconds) than the traveling time to the swapping

station [6]. Therefore, only the first part is considered in the following as the total travel cost, i.e., $P_{cost}^{v,k}$ is only related to the travel distance to the swapping station.

With GPS, the traveling path for GEV v to the swapping station in period k can be calculated based on the shortest path algorithm [10]. Denote the path length as $l_{v,k}$. Define the travel cost for GEV v in period k in terms of energy as $PC(l_{v,k})$, where $PC(\cdot)$ is a linear non-decreasing function to map the travel distance (or path length) to the travel cost in terms of energy [4], i.e.,

$$P_{cost}^{v,k} = PC(l_{v,k}), \qquad \forall v \in \mathbb{V}. \tag{4.11}$$

4.4 The Coordinated V2V (Dis)Charging Strategy

In this section, the V2V (dis)charging coordination problem is first formulated. Exploiting the Oligopoly game theory and Lagrange duality optimization techniques, the optimal decentralized solutions are derived.

4.4.1 V2V Charging Optimization Problems

Considering both the GEV discharging capabilities, charging demands and the electricity price, the V2V charging problem can be modeled as an Oligopoly game or a convex optimization problem in high demand case and supply surplus case, respectively:

- High Demand Case: When $\mathbb{P}_{\mathbb{S}} < \mathbb{P}_{\mathbb{D}}$, the problem can be solved in two steps. The first step is *decision making* in which the electricity price is determined by the supply side, (i.e., P_S^k or Eq. (4.4)). All the GEVs with surplus energy compete for discharging energy to maximize the individual discharging revenues, thus forming an Oligopoly game with the following objective.

$$\max_{u_k} R_{s,k}, \qquad \forall s \in \mathbb{S}. \tag{4.12}$$

  The problem constraints include (4.3), (4.8), (4.9), and (4.10). Based on the optimal price u_k^*, the individual discharged energy by GEV s is derived as $P_{s,k}^* = \frac{a}{b} - \frac{u_k^*}{b}$.

  The second step is *charging decision making* in which the GEVs with charging demands aim to minimize their charging cost based on the determined price u_k^* from (4.12).

$$\min_{P_{d,k}} \sum_{d \in \mathbb{D}} c_{d,k}. \tag{4.13}$$

  The optimization constraints include (4.1), (4.2), (4.5), (4.6), and (4.7).

- Surplus Supply Case: When $\mathbb{P}_{\mathbb{S}} \geq \mathbb{P}_{\mathbb{D}}$, the electricity price is determined by the demand side, (i.e., P_D^k or Eq. (4.2)). The problem is solved in two steps. *In the price decision making* step, all the demanding GEVs compete for charging forming an Oligopoly game, with the objective to minimize charging costs, i.e.,

$$\min_{u_k} c_{d,k}, \qquad \forall d \in \mathbb{D}. \tag{4.14}$$

The constraints include (4.1), (4.6), (4.7). Based on the optimal price u_k^*, the energy to be charged by GEV d is $P_{d,k}^* = \frac{a}{b} - \frac{u_k^*}{b}$.

In the discharging decision making step, based on the determined price, the discharging GEVs aim at maximizing revenues, i.e.,

$$\max_{P_{s,k}} \sum_{s \in \mathbb{S}} R_{s,k}. \tag{4.15}$$

The constraints include (4.3), (4.4), (4.5), (4.8), (4.9), and (4.10).

4.4.2 The Solutions of the Proposed Problems

In this section, the solutions to problems ((4.12), (4.13), (4.14), and (4.15)) are derived to obtain the optimal decisions for coordinated V2V charging strategy in the above two cases, respectively.

High Demand Case: In this case, the V2V charging problem can be solved in two steps.

4.4.2.1 Price Decision Making

The curve is given by $P_S^k = F(u_k) = \frac{a}{b} - \frac{u_k}{b}$ (since $u_k = a - bP_S^k$) where P_S^k is calculated by (4.4). Define U as the price satisfying $F(U) = 0$. The function $F(.)$ is twice continuously differentiable, strictly decreasing, and concave over the interval $[0, U]$.

To solve (4.12), two supplying GEVs i and j are taken as the simplest example to help understand the solving procedure [3]. GEVs i and j can choose supply functions simultaneously. For either GEV, given the discharged power by the other GEV, it first maximizes its own revenue. For instance, given $F^j(u_k)$ as the discharged power of GEV j at price u_k, the discharged power of GEV i, $F^i(u_k)$, can be expressed as $F(u_k) - F^j(u_k)$ because the total discharged power is a function of price u_k, i.e., $F(u_k)$. Then, GEV i will determine the optimal price to maximize its own revenue on its demand curve by solving $\max_{u_k} u_k[F(u_k) - F^j(u_k)] - C(F(u_k) - F^j(u_k))$, where

the discharging cost for GEV i, i.e., $C(F(u_k) - F^j(u_k))$, is given by $c_{i,k}$ as defined in (4.9). If the first order of the revenue is equal to zero at price u_k, i.e.,

$$\frac{d\{u_k[F(u_k) - F^j(u_k)] - C(F(u_k) - F^j(u_k))\}}{du_k}|_{u_k} = 0. \tag{4.16}$$

and $F^{j''}(u_k) \geq 0$ also holds at price u_k, u_k is a locally optimal price in maximizing the revenue for GEV i. Similarly, for GEV j, if the first order of the revenue equals to zero, and the second order $F^{i''}(u_k) \geq 0$, u_k is a locally optimal price in maximizing the revenue of GEV j. If we extend $F^i(.)$ and $F^j(.)$ linearly over $[0, U)$, the globally optimal price $u_k{}^*$ can be found in maximizing the revenues for both GEVs. This global optimal solution is unique due to the strict monotonicity of the demand function [3]. Similarly, the solving approach can be applied to the case with more than 2 GEVs.

4.4.2.2 Charging Decision Making

Having achieved the charging price u_k^*, the problem (4.13) is then solved to minimize the overall charging cost. The problem (4.13) has a convex objective function and linear constraints. Leveraging the Lagrange duality [11], a decentralized optimal solution can be achieved to (13). The basic principle is to integrate the constraints of problem (4.13) into the objective function by adding a weighted sum of all the constraint functions. Defined the Lagrangian function $L(.)$ for problem (4.13) as

$$\begin{aligned} &L(P_{d,k}; \lambda, \gamma, \iota, \varsigma, \zeta) = \\ &\sum_{d\in D} c_{d,k} - \sum_{d\in D} \lambda_d P_{d,k} + \sum_{d\in D} \gamma_d (P_{d,k} - P_{d,k}^{\max}) + \iota(\sum_{s\in S} \eta_s P_{s,k} - \sum_{d\in D} \eta_d P_{d,k}) \\ &- \sum_{d\in D} \varsigma_d (E_{d,k}^{init} + (a \cdot \eta_d P_{d,k} - P_{cost}^{d,k})) + \sum_{d\in D} \zeta_d (E_{d,k}^{init} + (a \cdot \eta_d P_{d,k}) - C_{battery}^{\max}) \end{aligned} \tag{4.17}$$

where λ_d, γ_d, ι, ς_d, and ζ_d are the Lagrange multipliers corresponding to constraints (4.1), (4.5), and (4.6), respectively. First minimize Lagrangian $L(.)$ over $P_{d,k}$. Define $D(\lambda_d, \gamma_d, \iota, \varsigma_d, \zeta_d)$ as the minimum value of $L(.)$ over $P_{d,k}$. Then, by maximizing the Lagrangian dual function $D(\lambda_d, \gamma_d, \iota, \varsigma_d, \zeta_d)$ over the Lagrange multipliers, the optimal solutions of (4.13) can be achieved, as shown below.

$$\begin{aligned} &\max_{\lambda_d, \gamma_d \iota, \varsigma_d, \zeta_d} D(\lambda_d, \gamma_d \iota, \varsigma_d, \zeta_d) \\ &s.t.\ \lambda_d, \gamma_d \iota, \varsigma_d, \zeta_d > 0. \end{aligned} \tag{4.18}$$

Surplus Supply Case: In this case, the solutions of (4.14) and (4.15) are obtained with a similar approach as (4.12) and (4.13) in the high demand case, respectively.

In the *price decision making* step, the electricity price is obtained through competition among the demanding GEVs to minimize the individual charging cost. Thus, we model the price decision problem into a single-step Oligopoly game

problem with all linear constraints for (4.14). By solving this Oligopoly problem (with a similar approach as that to (4.12)), the optimal price can be achieved. Then, in the *discharging decision making* step, given the optimal price, (4.15) is to maximize the total discharging revenues for the supplying GEVs. The maximization problem is a convex optimization problem with all linear constraints, which can be easily solved in a distributed manner exploiting Lagrange duality. The mathematical details are left for readers due to the similar procedure.

4.5 Performance Evaluations

In this section, the performance of the proposed V2V charging strategy is evaluated based on a customized simulator built in Matlab. The investigated performance metrics include: (1) discharged power and revenues of the supplying GEVs; and (2) charged power and charging costs of the demanding GEVs at the swapping station.

4.5.1 Simulation Setup

The GEV battery capacity is set to 60 KWh following the TESLA Model S [1]. The charging/discharging duration is set to 15 min for all the GEVs. The initial battery level for a GEV follows a uniform distribution over [10, 60]KWh. A highly realistic simulator, VISSIM [12], is employed to simulate a vehicular network with an area of 6000 m $*$ 2800 m. When the simulation starts, vehicles are pushed into the region from pre-set entries (e.g., 9 entries at the road ends), following a Poisson arrival process with a rate ζ (e.g., ζ = 2500 vehicles/hour/entry). After a certain warm-up duration t_ζ (e.g., 240 s), the vehicle pushing-in stops. The mobility information (e.g., locations, velocities, etc.) of vehicles can be recorded at the end of every simulation step (e.g., 0.2 s) into the trace files. Besides, the RSUs (e.g., with the number of 25) are deployed uniformly along the roads with a pre-defined transmission range (e.g., 150 m). The simulation is run over 3000 s.

4.5.2 Simulation Results of VANETs

First, the V2V charging strategy for the high demand case is examined, i.e., when the number of discharging GEVs is less than the number of demanding GEVs (e.g., 8 demanding GEVs in the setting). The results are shown in Fig. 4.3 where both the discharging performance of supplying GEVs and the charging performance of demanding GEVs are presented. In high demand case, the price is decided by supply side following an Oligopoly game among the supplying GEVs. It can be observed that both the total charged and discharged power increase when the number of

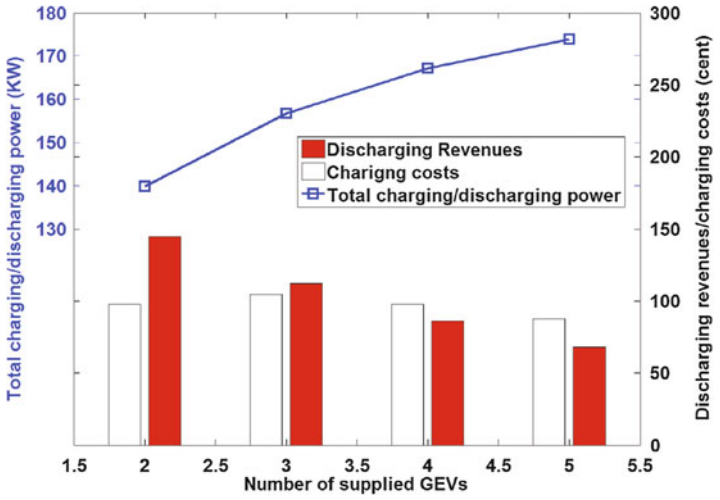

Fig. 4.3 (Dis)Charging performances for high demand case

supplying GEVs increases. Besides, the individual discharging revenues decrease when the discharged power increases due to the decreased price. In addition, the total discharged power is equal to the total charged power. Moreover, for the demanding GEVs, when the discharged power increases, the total charging cost first increases and then decreases. This can be explained as follows. When the amount of the discharged power is very small, e.g., only 2 supplying GEVs, the total available discharged power is low, resulting in a high energy price. If the discharged power increases by a little bit (e.g., from 2 to 3 supplying GEVs), the charging cost will increase first due to the increased productivity between the increased total energy and the slightly dropped price. However, with more power supply (e.g., 5 supplying GEVs), the energy price is significantly decreased and becomes dominant over the increase of total charged power, leading to reduces costs.

Then, the charging/discharging performance for the supply surplus case is given in Fig. 4.4, where 8 discharging GEVs is used in the setting. It can be seen that the total charged power is still equal to the total discharged power at the swapping station. Besides, the charging cost decreases when the total charged power increases, due to the reduces energy price. In addition, the discharging revenues decrease when the total charged power is increased due to the reduced electricity price.

4.6 Related Works

There have been abundant works studying the coordinated EV charging strategies from the aspect of G2V. For instance, in [7] and [13], the proposed strategies coordinate the charging duration and rates for a group of EVs to maximize the

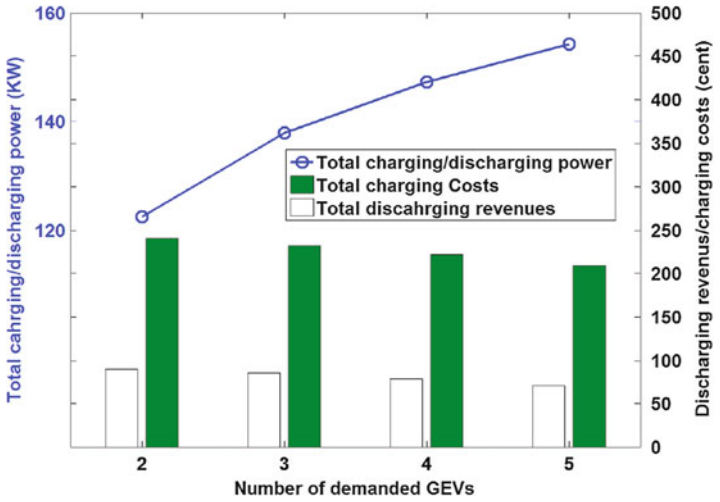

Fig. 4.4 (Dis)Charging performances for supply surplus case

total energy utilization of the power system. However, the high penetration levels of GEV impose high charging demands on the power grid, which can significantly affect the power system by causing voltage and frequency fluctuations [14]. Besides, the deployment of the fast-charging stations is costly [2]. To this end, more efficient and economic charging approaches need to be investigated.

With bi-directional chargers equipped with GEVs, GEVs can in turn supply energy to the grid, i.e., V2G. In this way, the voltage and frequency fluctuations in the power grid can be effectively regulated. For example, in [15] and [16], GEVs act as smart mobile storage devices to enable fast and accurate response to frequency and spinning reserves in maintaining the voltage and frequency stability. More importantly, energy can be transferred among GEVs at swapping stations without through the power grid, i.e., V2V charging [2]. V2V transaction provides a promising charging concept, by offloading high GEV charging demands from the power system to GEVs with surplus energy. Besides, swapping stations are much cheaper than the charging stations, yet with little transmission and power loss. Therefore, V2V energy transactions can significantly improve the GEV charging efficiency.

4.7 Conclusions

In this chapter, a semi-distributed V2V charging strategy has been developed for GEVs at the swapping station. A heterogeneous wireless network that integrates both VANETs and cellular networks has been proposed for delivering real-time information required by the V2V strategy. The proposed V2V charging strategy

aims to maximize the discharging revenues and minimize the charging costs, through Oligopoly game theory and Lagrange duality optimization techniques. Simulations results have demonstrated the performance of the proposed V2V charging strategy. In our future work, we intend to collect large-scale realistic vehicle traffic traces, to further verify the benefits of the proposed strategy in various and practical scenarios.

References

1. TESLA Motors, http://www.teslamotors.com/Pages/goelectric#
2. C. Liu, K. Chau, D. Wu, S. Gao, Opportunities and challenges of vehicle-to-home, vehicle-to-vehicle, and vehicle-to-grid technologies. Proc. IEEE **101**(11), 2409–2427 (2013)
3. J. Friedman, *Oligopoly and the Theory of Games* (North-Holland, Amsterdam/New York, 1977)
4. M. Wang, H. Shan, R. Lu, R. Zhang, X. Shen, Real-time path planning based on hybrid-VANET-enhanced transportation system. IEEE Trans. Veh. Technol. **64**(5), 1664–1678 (2014)
5. R. Zhang, Z. Zheng, M. Wang, X. Shen, L. Xie, Equivalent capacity in carrier aggregation-based LTE-A systems: a probabilistic analysis. IEEE Trans. Wirel. Commun. **13**(11), 6444–6460 (2014)
6. A. Abdrabou, W. Zhuang, Probabilistic delay control and road side unit placement for vehicular ad hoc networks with disrupted connectivity. IEEE J. Sel. Areas Commun. **29**(1), 129–139 (2011)
7. P. Richardson, D. Flynn, A. Keane, Local versus centralized charging strategies for electric vehicles in low voltage distribution systems. IEEE Trans. Smart Grid **3**(2), 1020–1028 (2012)
8. T. Kristoffersen, K. Capion, P. Meibom, Optimal charging of electric drive vehicles in a market environment. J. Appl. Energy **88**(5), 1940–1948 (2011)
9. J. Escudero-Garzas, G. Seco-Granados, Charging station selection optimization for plug-in electric vehicles: an oligopolistic game-theoretic framework, in *Innovative Smart Grid Technologies*, Washington, DC, 2012
10. M. Abboud, L. Jaoude, Z. Kerbage, Real time GPS navigation system (2004), http://webfea-lb.fea.aub.edu.lb/proceedings/2004/SRC-ECE-27.pdf
11. S. Boyd, L. Vandenberghe, *Convex Optimization* (Cambridge University Press, Cambridge/New York, 2004)
12. http://vision-traffic.ptvgroup.com/en-uk/products/ptv-vissim/
13. M. Wang, H. Liang, R. Zhang, R. Deng, X. Shen, Mobilty-aware coordinated charging for electric vehicles in VANET-enhanced smart grid. IEEE J. Sel. Areas Commun. **32**(7), 1344–1360 (2014)
14. M.F. Shaaban, M. Ismail, E.F. El-Saadany, W. Zhuang, Real-Time PEV Charging/Discharging Coordination in Smart Distribution Systems, IEEE Trans. Smart Grid **5**(4), 1797–1807 (2014)
15. K. Thirugnanam, T. Joy, M. Singh, P. Kumar, Modeling and control of contactless based smart charing station in V2G scenario. IEEE Trans. Smart Grid **5**(1), 337–348 (2014)
16. N. Machiels, N. Leemput, F. Geth, J. Roy, J. Buscher, J. Driesen, Design criteria for electric vehicle fast charge infrastructure based on flemish mobility behavior. IEEE Trans. Smart Grid **5**(1), 320–327 (2014)

Chapter 5
Conclusions and Future Directions

5.1 Concluding Remarks

In this monograph, the EV mobility has been incorporated into the EV fast charging/discharging coordination framework, which is the most distinct feature of the vehicles. VANET-enhanced coordinated EV charging strategy has been developed to improve the overall energy utilization subject to the charging load capacity at charging stations and cut down the EV travel cost while preventing the power system from overloading. Specifically, a VANET-enhanced smart grid architecture with real-time vehicle information collection capabilities has been introduced to deliver the required messages among the vehicles and RSUs. Then, two EV charging strategies, i.e., the predictive mobility-aware coordinated EV charging strategy and V2V energy swapping strategy, have been proposed with the objective to maximize the overall charging-energy-minus-travel-cost with avoiding the power overloading problem. Extensive simulations have been performed to evaluate the travel cost introduced by the transmission delay of VANETs. The results have further demonstrated that the proposed EV fast-charging strategy surpass the existing strategy that does not consider the EV mobility and travel cost in the performance metrics such as the total EV charging power, the average EV travel cost and the success ratio for the involved charging EVs.

5.2 Future Research Directions

For the potential future research directions, there still exist many challenging issues standing in the way to efficiently performing the charging applications for EVs. The issues to our most interest include how to select the optimal transmission network under different situations, how to balance the tradeoff between the system technical

M. Wang et al., *Mobile Electric Vehicles*, Wireless Networks,
DOI 10.1007/978-3-319-25130-1_5

limitations and drivers' preferences, and how to improve the business revenue model to better stimulate the EVs to achieve the win-win situation for both EVs, charging stations and the grid operators.

5.2.1 Network Selection for Real-Time Information Delivery

In VANETs, the V2V and V2R connections can be intermittent due to the vehicle mobility, which results in non-neglectable transmission delay and further additional travel cost. The cellular network can provide wide coverage for the vehicles, but the services for large-volume vehicle information delivery will considerably bring about additional monetary cost. Therefore, by combining both cellular networks and VANETs to form a heterogeneous wireless network with multiple radio access technologies, more efficient mechanisms for information delivery can be designed while reducing the communication costs, e.g., low deployment and operation costs. In such a heterogeneous wireless network, the network selection mechanism is desirable to strike the balance between the travel cost incurred the transmission delay in VANETs and the monetary service cost mainly brought by the cellular networks. Thus, in our future work, an intelligent and adaptive network selection mechanism is indispensable to decide the best access network for the vehicles in different conditions. The aim is to balance the travel cost from the transmission delay of VANETs and the monetary cost associated with the cellular transmissions, in order to achieve a more efficient and economic information collection and dissemination for the EV charging decision making.

5.2.2 Balancing the Tradeoff Between the System Technical Limitations and Preferences of the Drivers

Bearing the personal behaviors and the range anxiety due to the vehicle mobility, drivers usually have their own preferences when choosing a destination (e.g., a charging/swapping station). But sometimes the drivers' preferences may conflict with the situation that the preferred charging/swapping station may not be able to support any more power loads. In this situation, in order to avoid the overload of the smart grid, another charging/swapping station will be designated for EV v to charge or discharge, which is referred to as spatial coordination.

Since drivers tend to follow their individual preferences, a tradeoff exists between the optimal power utilization of the system (e.g., power system) and the individual satisfactions. This tradeoff raises the challenging issues of (1) how to define and model the preferences of individual drivers, taking into the typical human behaviors, and (2) how to balance the system limitations (e.g., overload avoidance) with drivers' preferences.

5.2.3 *Business Revenue Model for EVs and Extended Large-Scale Simulations*

The spatial and temporal coordination for fast EV charging raises additional challenges. The economic model built for EV interaction/negociation with the system need to benefit both the EVs and the system operators. Specifically, the economic model should define stimulation model to provide incentives for the drivers to use the designed applications or follow the received charging/discharging decisions.

In addition, we intend to employ large-scale realistic vehicle traffic traces to conduct more extensive simulations and validations in real-world scenarios, based on which we hope to find implications of how different factors can impact the network design and operations.